A PHASE SHIFT METER, ITS DESIGN AND PERFORMANCE

By

JOSEPH D. EISLER

Bachelor of Science

Massachusetts Institute of Technology

Cambridge, Massachusetts

1932

Submitted to the Faculty of the Graduate School of
the Oklahoma Agricultural and Mechanical College
in Partial Fulfillment of the Requirements
for the Degree of
MASTER OF SCIENCE
1954

A PHASE SHIFT METER, ITS

DESIGN AND PERFORMANCE

Thesis and Abstract Approved:

Herbert L. Jones
Thesis Adviser

David L. Johnson
Faculty Representative

Robert MacVicar
Dean of the Graduate School

PREFACE

Within the past several years, great technological strides have been made in the fields of Electrical Engineering and Electronics. The engineer engaged in these fields of endeavor is continuously called upon to perform more and more precise measurements of electrical response characteristics of numerous and varied components and devices. He is, therefore, of necessity forced to provide or improvise suitable equipment to carry out such measurements.

In general, the behavior of any electrical network, electrical or electromechanical device can be fully described in terms of amplitude and phase response to a steady state sinusoidal signal covering a broad frequency spectrum. While a number of precise and adequate schemes are available to carry out amplitude response measurements, the number and quality of phase measuring devices is correspondingly small and lacking in precision.

Recognizing this lack of availability of suitable precise phase measuring devices, the author of this thesis embarked upon the development of a Phase Shift Meter designed to fill this important gap in the realm of electrical measurements. The work reported herein was carried out as a research project by the author while employed in the Research Department of the Stanolind Oil and Gas Company, Tulsa, Oklahoma. The Phase Shift Meter, whose design and performance will be described in detail in the body of this thesis, has been instrumental in solving numerous problems in the design and performance of various electrical devices and networks and has been since its original development in continuous use by the various members of the Research Staff engaged in such work.

ACKNOWLEDGMENT

The author wishes to express his sincere appreciation to Professors H. L. Jones and D. L. Johnson, both of the Electrical Engineering Department of the Oklahoma Agricultural and Mechanical College, for their invaluable assistance and criticism in the preparation of this thesis. He is likewise greatly indebted to the Stanolind Oil and Gas Company for granting permission to publish this material.

TABLE OF CONTENTS

LIST OF TABLES

LIST OF ILLUSTRATIONS

Figure		Page

CHAPTER I

Introduction

At the inception of the art of Electrical Engineering, the measurement of phase angle was limited to power applications and effective phase measuring techniques[1] were developed concurrently with ever increasing use of alternating currents in power generation, transmission and use. As the art developed to include Telegraphy, Telephony, and Electronics, the necessity for precision and flexibility of phase measuring techniques grew.

Present day measurements technology offers the Electrical Engineer many and varied means for carrying out phase measurements by means of oscillographic and oscilloscopic techniques as well as by means of complex electronic instruments capable of indicating phase angle over a wide range of the frequency spectrum.

Particularly in the Electronics branch of the Electrical Engineering art, the measurement of phase angle assumed great importance in determining the behavior of characteristics of a variety of circuit components such as resistors, condensers, and inductors as well as of electrical, electromagnetic and electro-

---

[1] F. A. Laws, Electrical Measurements, p. 530

acoustic devices, including electrical filters, amplifiers, servo-mechanisms, and a host of other devices whose steady state and transient responses are of prime importance in their design and use.

Mathematical theories have been developed which not only relate the steady state response to the transient response[2] of a particular network or apparatus, but likewise relate the steady state amplitude response to the phase response or vice versa[3,4].

The measurement and knowledge of phase response is of extreme importance to the communication engineer, since having such information, he can predict the quality of performance of long transmission lines carrying voice and other signals. The measurement of phase likewise offers a very sensitive means for evaluating the performance and lining up of multichannel equipment of great variety in which identical response among the individual channels is one of the important specifications. Multichannel telemetering equipment belongs to this class.

In order to appreciate fully the significance of phase angle, or phase shift measurement, and its relation to electrical measurements in general, it is in order to define this quantity. Phase angle is defined as the magnitude and sign of the transit time of

---

[2] V. Bush, Operational Circuit Analysis, p. 181

[3] H. Bode, Network Analysis and Feedback Amplifier Design, p. 312.

[4] Ibid. p. 320.

a steady state sinusoidal signal of a particular frequency between the input and output terminals of a network. The transit time may be positive (lag) or negative (lead) and is caused, broadly speaking, by the temporary storage and/or release of electrical energy by the various circuit parameters comprising such a network. This transit time, if related to the period of the sinusoidal signal, can be expressed in electrical degrees. Thus, for any particular frequency, the time delay is given by

$$t = \frac{\theta}{360f} \qquad (1)$$

where t - delay in seconds

θ - phase angle in degrees

f - frequency in cycles per second

Expressed differently, the phase angle is proportional at any given frequency to the time difference between corresponding phase points on the sinusoidal input and output signals.

One of the most commonly employed methods in measuring phase of phase difference is the oscilloscope method[5,6]. While this method is simple and reliable from the instrumental point of view, it nevertheless suffers seriously from lack of precision, particularly

---

[5]J. L. Glaser, "Accurate Phase Difference by Lissajous Figures," Electronics, II (March, 1952), p. 206.

[6]R. G. Manley, Waveform Analysis, p. 243.

when the difference in phase between two quantities lies in the neighborhood of $\pm \frac{n\pi}{2}$ where n is an odd integer. A number of variants are available which attempt to circumvent this difficulty[7]. But these again are capable of determining phase angle to approximately $\pm 5°$ up to frequencies of about 4 kilocycles.

With the rapid advance of the electronic art, a need arose for a precise measurement of phase angle over a broad range of the frequency spectrum by direct meter indicating means. Frequently, the measurements have to be performed on circuits of high impedance and at low power levels. Therefore, the phase indicating meters are designed to produce minimum loading of the circuits under test. Phase shift measurement precision requirements are often of the order of one electrical degree. Oftentimes it is necessary to visualize the shape of the entire phase shift characteristic over a relatively wide band of frequencies such as, for example, the phase characteristic of a filter network; therefore, it is desirable to employ phase measuring instruments which are substantially independent of amplitude variation of the input or the output signals over the band of frequency of interest. This requires that the instrument undergo a minimum of adjustment throughout the measurement. Direct phase reading

---

[7]W. R. McLean and L. V. Sivian, "Direct Reading Audio Phase Meter," Journal of Acoustical Society of America, 25 (April, 1931), p. 419.

devices are likewise preferable which do not involve the necessity of computation or interpretation.

With these ideas in mind, the author of this thesis was able to design a suitable electronic phase meter which meets the above specifications in almost every respect. The phase shift meter to be described was designed specifically for sub-audio and audio range and its performance, with some slight modifications, could relatively easily be extended into supersonic range.

CHAPTER II

Principle of Operation

The phase shift meter under discussion is designed for determining the phase <u>difference</u> between two sinusoidal voltages of like frequency. The principle of this meter is as follows: If two sinusoidal vector voltages V_1 and V_2, which are displaced from each other in time phase by an angle θ, are subtracted vectorially, then their difference by the law of cosines is

$$V_{diff} = \sqrt{V_1^2 + V_2^2 - 2V_1V_2 \cos \theta} \qquad (2)$$

If V_1 and V_2 are not only made equal to each other, but also equal to a certain preselected magnitude V_o so that $V_1 = V_2 = V_o$ then,

$$V_{diff} = 2V_0 \sqrt{\frac{1 - \cos \theta}{2}} \qquad (3)$$

from which

$$V_{diff} = 2V_o \sin 1/2\ \theta \qquad (4)$$

The vector representation of this operation is shown in Figure 1a.

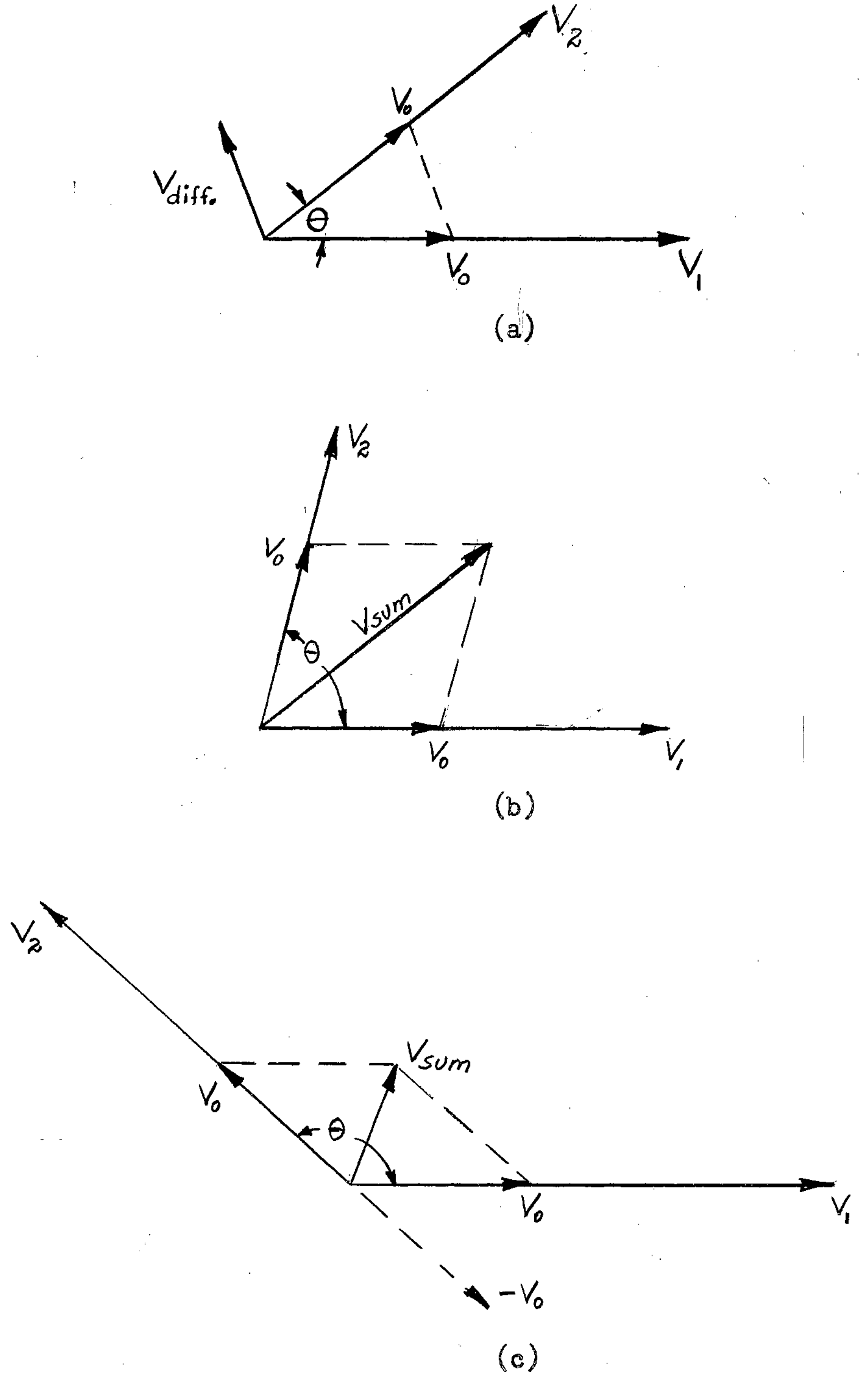

Figure 1. Vector Relations used in Measuring Phase Angle.

If, however, V_1 and V_2 are added vectorially, their sum will be

$$V_{sum} = \sqrt{V_1^2 + V_2^2 - 2V_1V_2 \cos (180-\theta)} \qquad (5)$$

Furthermore, if $V_1 = V_2 = V_o$, as before

$$V_{sum} = 2V_o \sqrt{\frac{1 + \cos \theta}{2}} \qquad (6)$$

from which

$$V_{sum} = 2V_o \cos 1/2\, \theta \qquad (7)$$

The vector representation of this operation is shown in Figure 1b.

By proper choice of magnitude V_o, the design of the indicating meter scale and its calibration are immediately established. However, if equation (4) were solely used for establishing this calibration, the meter scale would be unduly compressed for phase angles θ lying close to $\pm \pi$. For this reason relation (4) is used for angles lying between 0 and $\pm \frac{\pi}{2}$ radians and relation (7) for angles lying between $+ \frac{\pi}{2}$ and $+ \pi$ or between $- \frac{\pi}{2}$ and $- \pi$. The vector diagram for the example of the latter case is shown in Figure 1c. Using such a scheme, a single calibration scale may be used for the <u>sum</u> and the <u>difference</u> of V_1 and V_2 (both adjusted to magnitude V_o) covering all quadrants. The calibration of the indicating meter is so chosen as to give full scale deflection when θ corresponds to $\pm \frac{\pi}{2}$, $\pm\frac{3\pi}{2}$, $\pm \frac{5\pi}{2}$ etc. radians and zero scale deflection when θ is equal to 0, $\pm \pi$, $\pm 2\pi$, $\pm 3\pi$, etc. Since

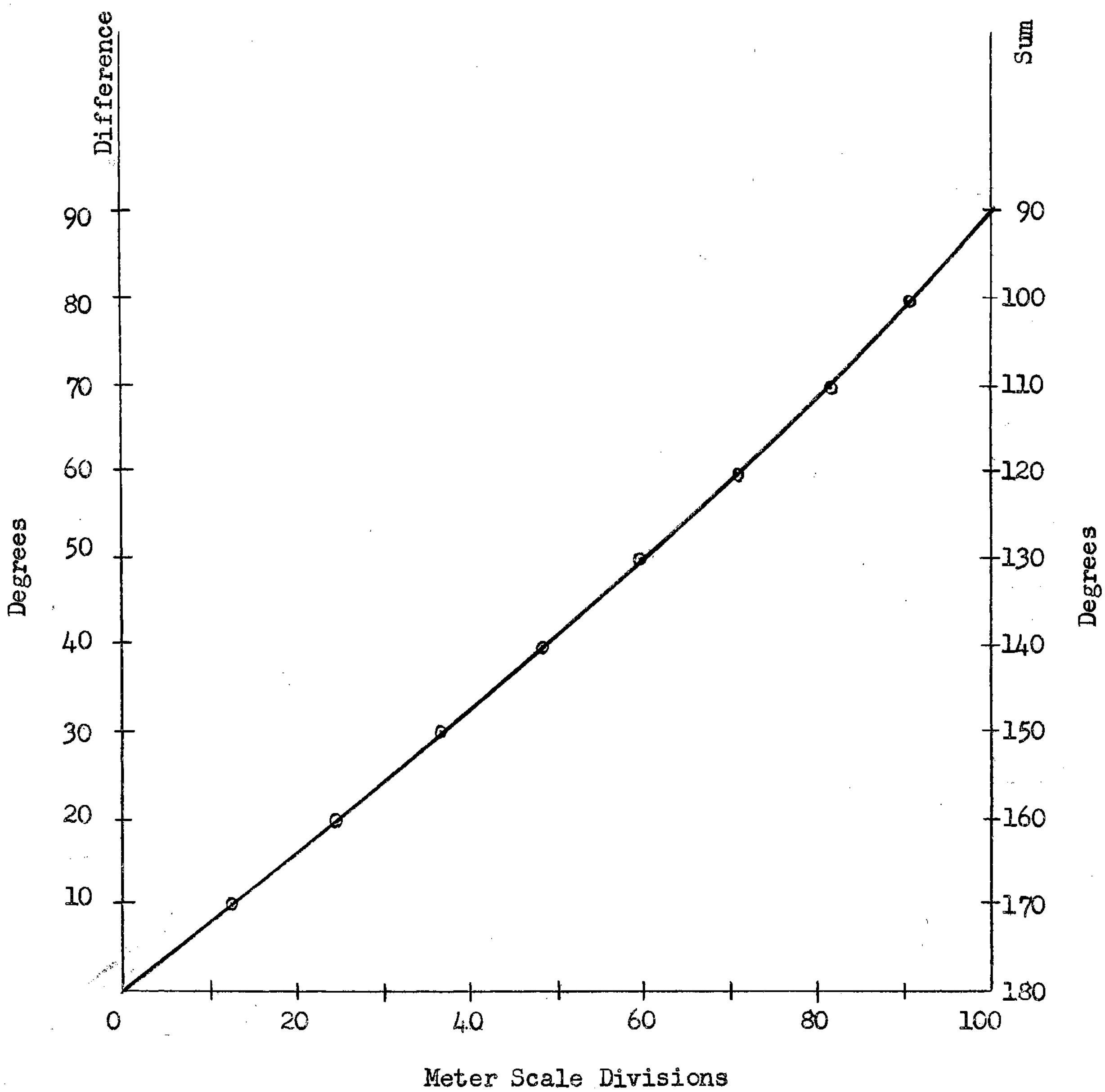

Figure 2. Theoretical Calibration of the Phase Shift Meter Scale.

only half angles of the actual phase difference between V_1 and V_2 are determined, the scale is compressed at its upper end by approximately 30%. Such a theoretical scale calibration is illustrated in Figure 2. While the plot describes the indicating meter deflection for phase angles in the first and second quadrants, identical characteristic is valid for phase angles in the third and fourth quadrants. For this case, the right ordinate is used for the angles in the third quadrant and the left ordinate for the angles in the fourth quadrant. Since in the design of the phase meter the vector sum or vector difference of a.c. voltages V_1 and V_2 is rectified to permit the use of a sensitive d.c. microammeter for final phase angle indication, the actual calibration characteristic departs slightly from the ideal given in Figure 2.

The principle of operation of the phase shift meter can be most easily understood by reference to the basic block diagram presented in Figure 3. Here, the two sinusoidal voltages V_1 and V_2 having a phase shift angle Θ between them are fed separately to two identical automatic control circuits A_1 and A_2 which compensate precisely for the variations in magnitudes of V_1 and V_2 as a function of frequency. For example V_1 may be an input voltage to a network or an apparatus and V_2 the output voltage. These equalized voltages are then suitably attenuated by manually adjustable potentiometers P_3 and P_4 so that $V_1 = V_2 = V_o$, where V_o is again a certain preselected magnitude designed to make the

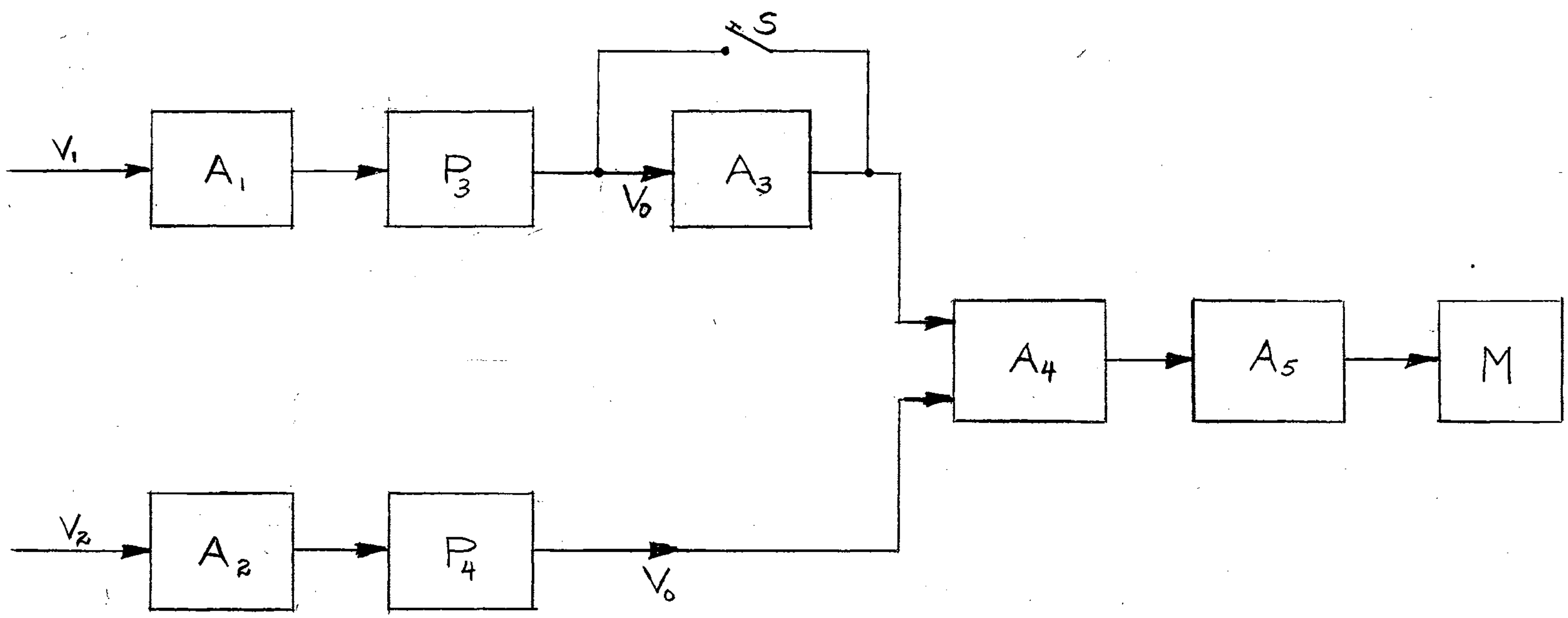

Figure 3. Basic Block Diagram of the Phase Shift Meter.

indicating precalibrated meter scale read directly in degrees phase. One of the equalized vector voltages V_2 is fed directly to a mixer amplifier stage A_4 and thence through a full wave rectifier circuit A_5 to a d.c. indicating meter M. The other vector voltage V_1 upon equalization by the automatic control stage A_1 and potentiometer P_3 is fed to an inverter stage A_3 of unity gain to the mixer stage A_4 and thence to a full wave rectifier A_5 and indicating meter M. The inverter stage is inserted into the circuit by means of switch S only when the difference of two vector voltages is read on the indicating meter and is bypassed again by means of switch S when the sum of the two vectors is read on the indicating meter. The "difference" or the "sum" position of switch S is determined at any frequency, automatically, by noting the deflection of the indicating meter M. The possible ambiguity between the first and fourth and again between the second and third quadrants is avoided by inspection of the circuit or the device under test and determining the expected phase shift either at low or high end of the operable frequency spectrum and then following the deflection of the meter either up or down the angle scale as a function of frequency. Frequently, it is possible to determine zero phase shift from the circuit considerations, e.g. at resonance and departing from that point either up or down on the setting of the test oscillator supplying the input signal to the network or the device under test. Methods likewise exist by means of which it is possible to determine whether the phase angle is leading or lagging, but this will be discussed at length in a subsequent chapter.

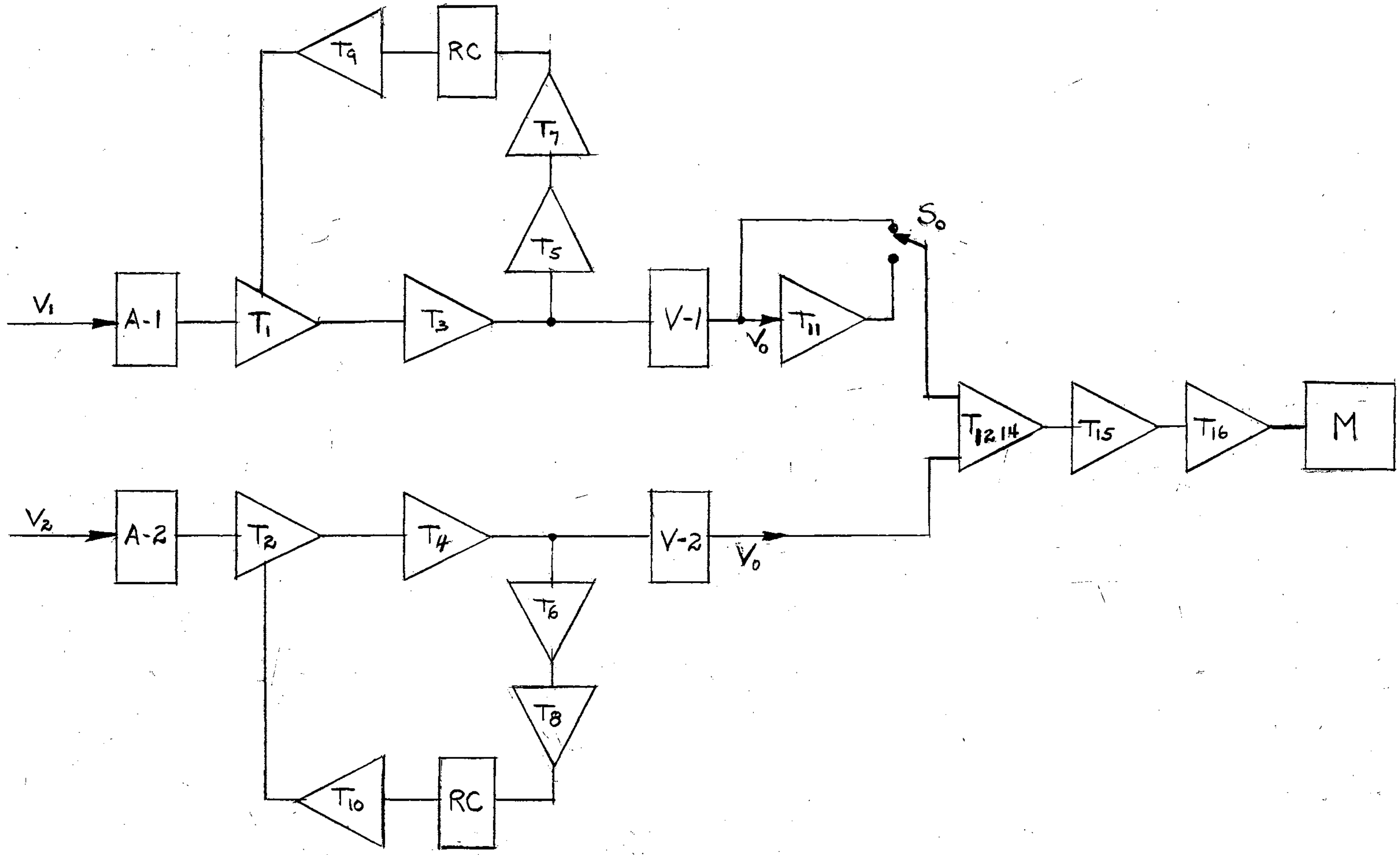

Figure 4. Schematic Block Diagram of the Phase Shift Meter.

CHAPTER III

Circuit Diagram and Physical Embodiment of the Instrument

Before proceeding with the detailed description of the actual wiring diagram of the instrument, it is helpful to consider a functional block diagram shown in Figure 4. This diagram is a further amplification of the basic block diagram shown in Figure 3, and includes certain pertinent portions of the instrument which are necessary to its satisfactory operations. In particular, the automatic volume control feedback loops are shown which equalize the variable magnitudes of input voltages V_1 and V_2 which are then manually adjusted to a voltage V_o This voltage is kept substantially constant throughout the phase shift measurement.

The automatic volume control circuits involve an identical pentode input stage T_1 (or T_2) for each of the two channels of the device. The transconductance of this stage is varied by changing the suppressor bias. This stage, therefore, represents the control element in the negative feedback loop of the control circuit. This control stage is followed by additional a.c. amplification, stage T_3(or T_4). The negative feedback portion of the automatic control circuit consists of an a.c. amplifier stage T_5(or T_6) a half wave rectifier T_7(or T_8), an R.C. filter, and a stage of a d.c. amplifier T_9(or T_{10}). The voltage output of the latter is impressed on the suppressor electrode of the control stage T_1(or T_2). The action of the automatic volume control will be treated at length in Chapter V. The remaining portions of the block diagram are identical to those shown in Figure 3, and consist of an inverter stage T_{11} of unity gain in one of the channels, a mixer stage T_{12} and T_{14}, driver stage T_{15}, a full wave rectifier stage T_{16} and an indicating d.c. meter M.

The complete wiring diagram is shown in Figure 5 and the various portions thereof can be directly related to the block diagram in Figure 4. The circuit parameter values used in this design are listed in Table I. There are, however, two features which require further explanation. One of these are potentiometers A-1 and A-2 and the second is a mechanically ganged switch labeled S_1 S_2 S_3. The purpose of potentiometers A-1 and A-2 is to prevent overload and grid rectification of the input stages T_1 and T_2. These potentiometers are set manually at the beginning of phase measurement and the input level is determined on the indicating meter for either or both input signals. The input level for each channel, as well as the value of adjusted magnitude V_o for each channel is applied to the respective inputs of mixer stage T_{12} T_{14} by means of ganged selector switches

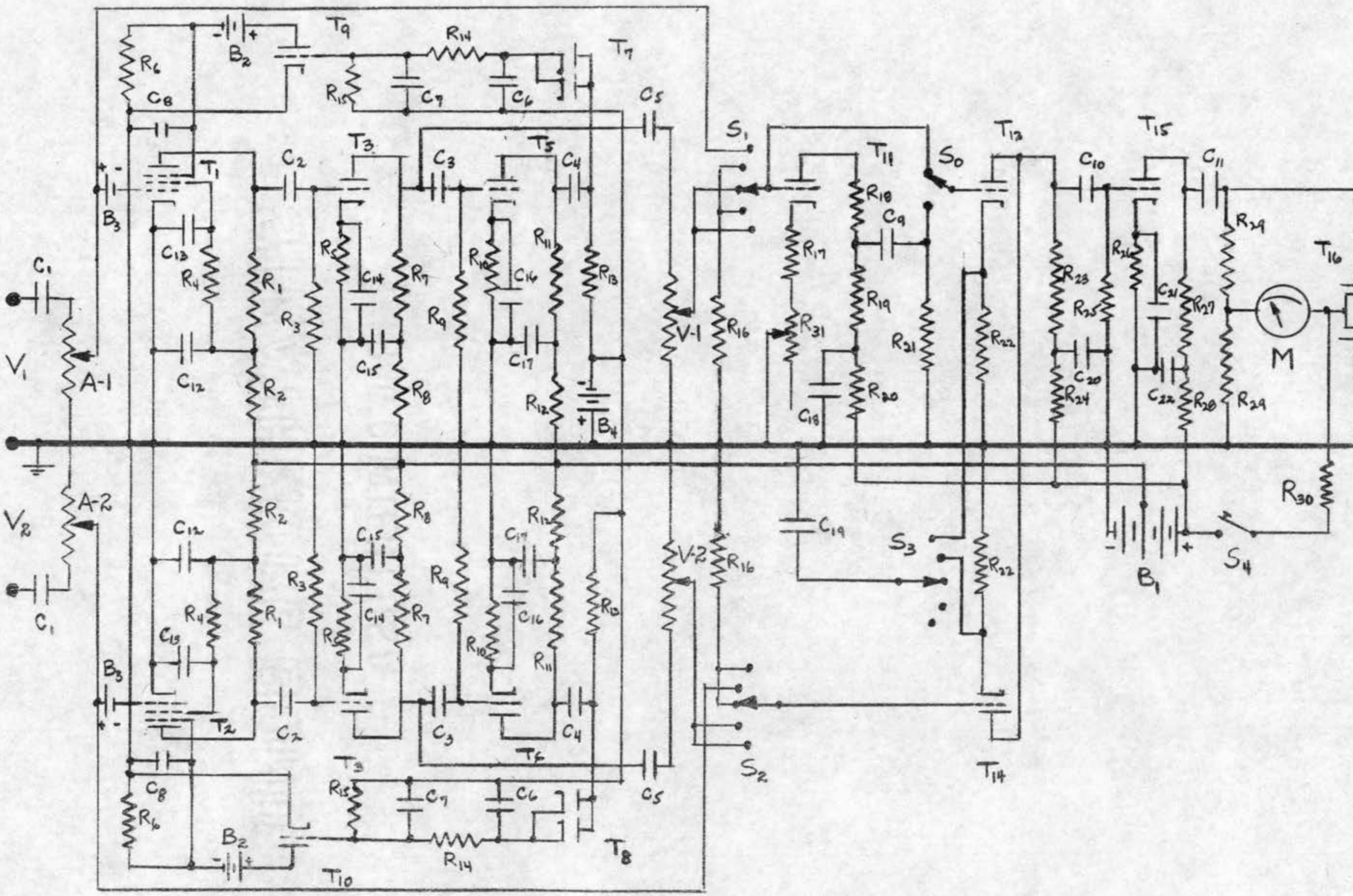

Figure 5. Circuit Diagram of the Phase Shift Meter.

TABLE I

List of Components

R_1	-	500K	R_{20}	-	20K	C_4	-	1.0 mfd.
R_2	-	20K	R_{21}	-	1000K	C_5	-	0.75 mfd.
R_3	-	2000K	R_{22}	-	5K	C_6	-	8.0 mfd.
R_4	-	2000K	R_{23}	-	100K	C_7	-	8.0 mfd.
R_5	-	10K	R_{24}	-	20K	C_8	-	6.0 mfd.
R_6	-	50K	R_{25}	-	1000K	C_9	-	0.5 mfd.
R_7	-	100K	R_{26}	-	5K	C_{10}	-	0.25 mfd.
R_8	-	20K	R_{27}	-	100K	C_{11}	-	4.0 mfd.
R_9	-	2000K	R_{28}	-	20K	C_{12}	-	8 mfd.
R_{10}	-	10K	R_{29}	-	250K	C_{13}	-	8 mfd.
R_{11}	-	100K	R_{30}	-	3900K	C_{14}	-	25 mfd.
R_{12}	-	20K	R_{31}	-	10K Pot.	C_{15}	-	8 mfd.
R_{13}	-	500K	A-1	-	1000K Pot.	C_{16}	-	25 mfd.
R_{14}	-	250K	A-2	-	1000K Pot.	C_{17}	-	8 mfd.
R_{15}	-	2000K	V-1	-	100K Pot.	C_{18}	-	8 mfd.
R_{16}	-	100K	V-2	-	100K Pot.	C_{19}	-	25 mfd.
R_{17}	-	15K	C_1	-	0.5 mfd	C_{20}	-	8 mfd.
R_{18}	-	100K	C_2	-	0.03 mfd	C_{21}	-	50 mfd.
R_{19}	-	100K	C_3	-	0.03 mfd	C_{22}	-	8 mfd.

TABLE I (Continued)

T_1, T_2	- 6J7
T_3, T_5	- 6C8-G
T_4, T_6	- 6C8-G
T_7, T_8	- 6H6
T_9, T_{10}	- 6C5
T_{11}, T_{12}	- 6C8-G
T_{14}	- 1/2 6C8-G
T_{15}	- 76
T_{16}	- 6H6
B_1	- 90 volts & 135 volts
B_2	- 45 volts
B_3	- 1-1/4 volts
B_4	- 6 volts

Note: Condenser C_1 to C_{11} inclusive - paper or mica;
Condensers C_{12} to C_{22} inclusive - electrolytic.

S_1 S_2 S_3 in the following sequential switching: Switch position No. 1 connects voltage V_1 to the grid of T_{12}; switch position No. 2 connects voltage V_2 to the grid of T_{14}; switch position No. 3 monitors the adjusted value V_o of channel No. 1 by connecting it to the grid of T_{12}; switch position No. 4 monitors the adjusted value V_o of channel No. 2 by connecting it to the grid of T_{14}; switch position No. 5 combines the adjusted voltages in the mixer stage T_{12} T_{14} for phase difference determination. A separate switch S_o selects either the sum or the difference of two voltages depending upon the magnitude of the phase angle.

The instrument is self contained and is entirely battery powered to eliminate difficulties with power line frequency pickup. This is particularly advantageous when phase shift measurements are being performed on circuits operating at low levels. This feature also permits the use of such an instrument outside the laboratory or under field conditions. The internal construction is presented in Figures 6 and 7 which shows the top and the bottom view of the chassis, respectively. Figure 8 shows the outside view of the instrument with all controls conveniently mounted on the sloping front panel. A screw driver adjustment is provided for setting the gain of the inverter stage to exactly unity. Figure 9 shows a close-up view of the indicating meter which is, in this case, a 50 microampere d.c. meter manufactured by Sensitive Instrument Research Corporation.

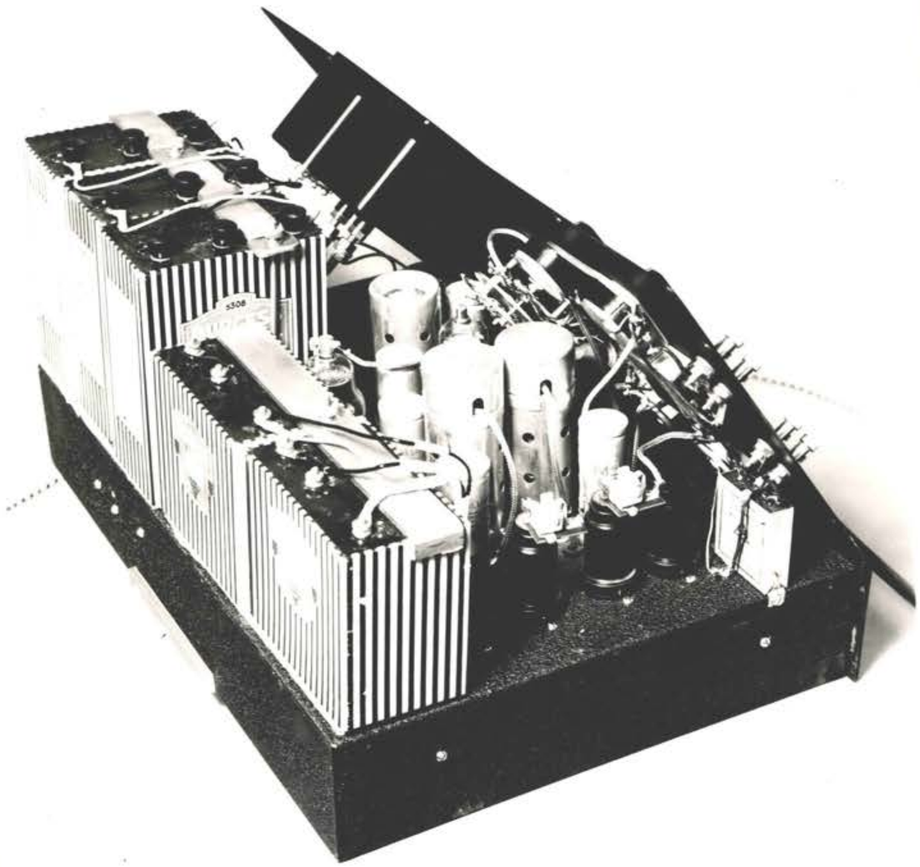

Figure 6. Top View of Phase Shift Meter Chassis.

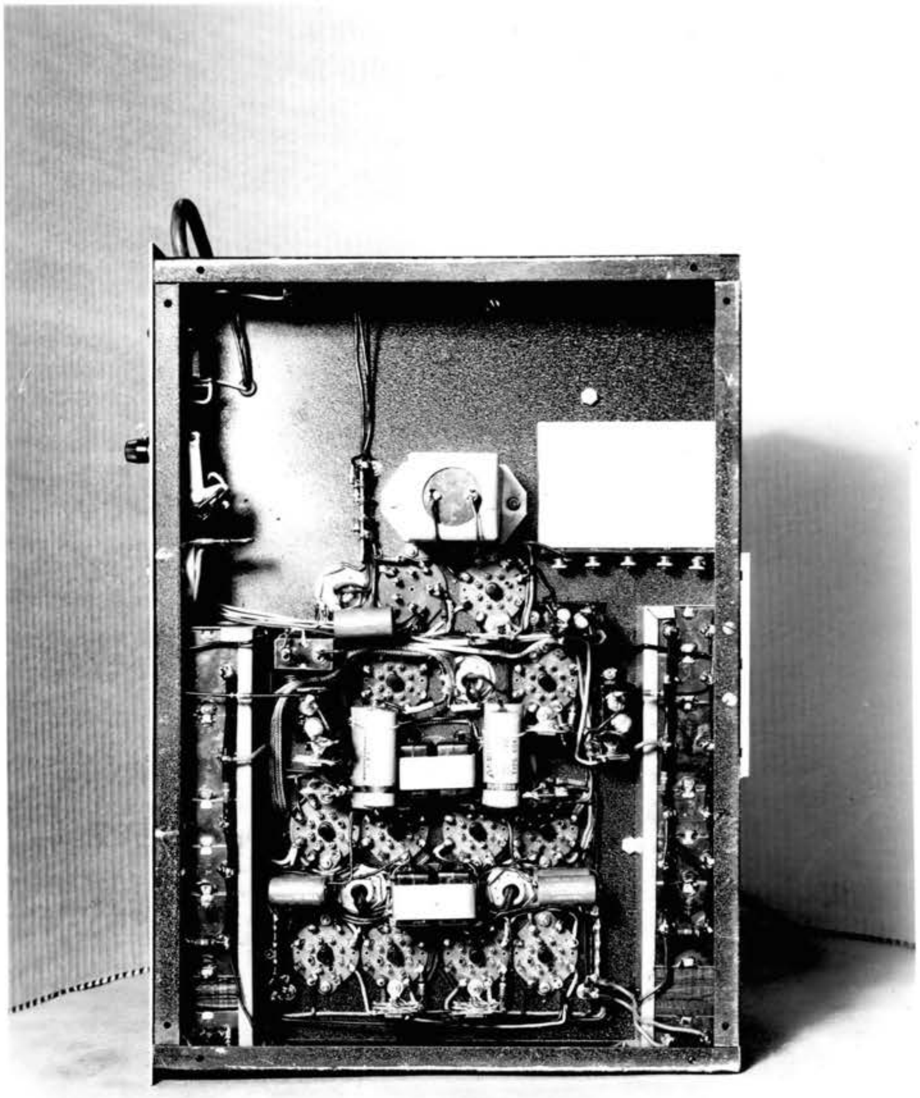

Figure 7. Bottom View of the Phase Shift Meter Chassis.

Figure 8. Front View of the Phase Shift Meter.

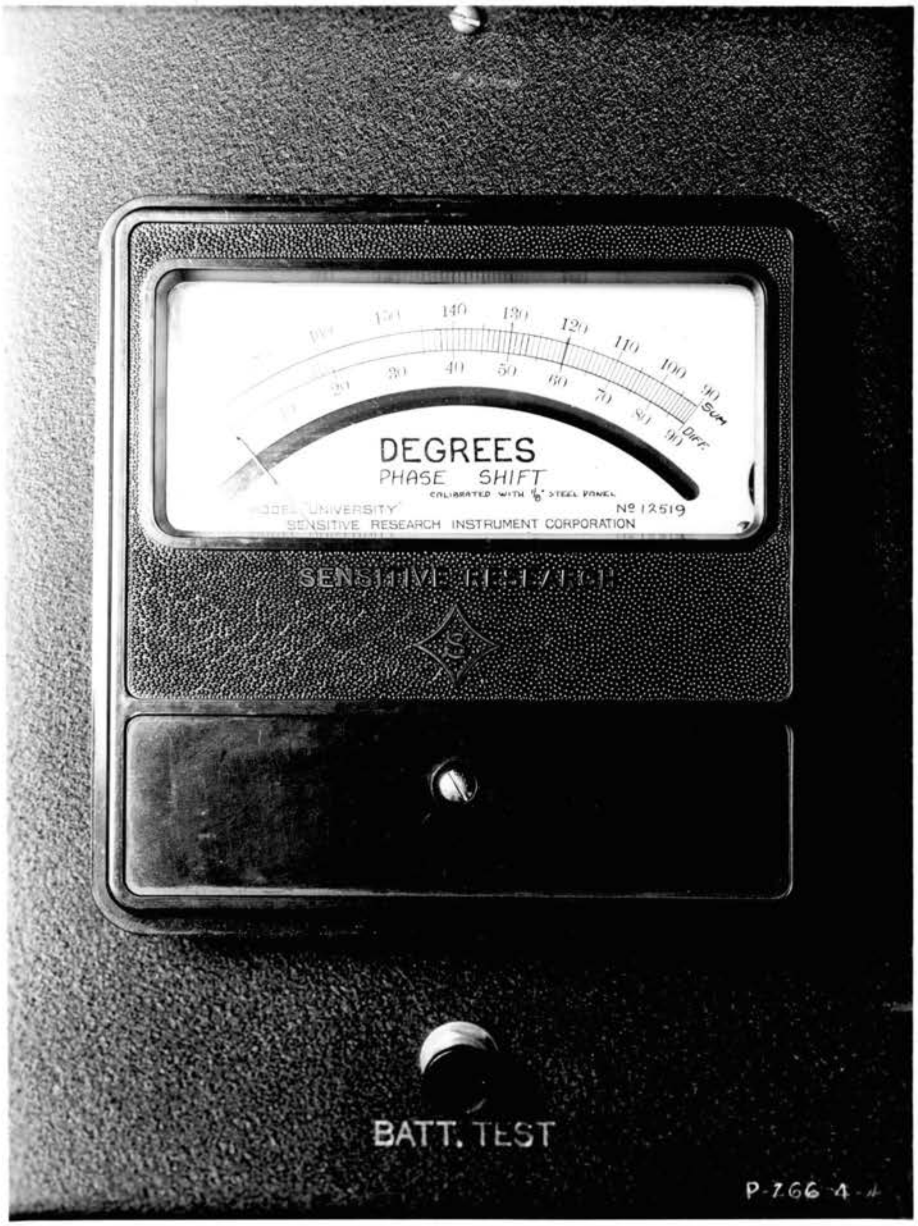

Figure 9. Close-Up View of the Phase Shift Meter Scale.

The degrees scale was prepared by the manufacturer on a special order according to the calibration supplied. It may be seen that phase angle of the order of one electrical degree or better can be easily read. A battery test push button S_4 is provided which checks the "B" battery voltage. Filaments are normally supplied by an external 6-volt storage battery. Under normal operating conditions one of the input terminals of both channels is at ground potential. This arrangement is generally satisfactory when measuring phase shift characteristics of amplifiers on other four terminal networks having a common low or ground bus. In those cases when the four terminal networks have all four terminal independent electrically, isolation transformer must be inserted into one of the channels of the phase meter. In such a case the phase characteristics of the transformer is determined as a function of frequency and algebraically subtracted from the overall phase measurement. The input impedance of the meter is 1 megohm for the range of frequencies for which the meter was designed.

CHAPTER IV

Operational Procedure

At the start of phase shift measurement, the filament leads of the phase meter are connected across a 6-volt storage battery without regard to polarity. The meter is then turned on by means of main power switch which not only completes the filament circuit, but also connects the main 135 volt "B" battery. (See Figure 8 for location of the various control knobs). Battery test push button is next operated. This tests the condition of the main "B" battery. The reading of the meter should come up to the red mark on the meter face. The red mark is placed opposite 60° on the difference scale and is used for certain other settings of controls prior to the phase measurement. The circuit under test is connected to the input terminals of Channel I and Channel II, observing the polarity with respect to the grounded terminals (lower post of each input pair). The input voltage to the circuit under test may be connected to Channel I and the output voltage of the circuit to Channel II, or vice versa. The main selector switch is placed in position marked A-1. The frequency of the source supplying the sinusoidal voltage to the circuit or the device under test is varied over the required range. Control A-1 is adjusted so that at no time does the deflection of pointer of the meter exceed full scale meter deflection. The main selector switch is placed into position marked A-2 and the above process is repeated. In this case, however, the control knob marked A-2 is varied until the maximum deflection of the meter does not exceed full scale meter deflection. These two adjustments normally take a very short time and their purpose is to keep the levels of the input signals to both channels of the Phase Meter within safe levels so as not to overload the various amplifying stages. Next step is to place the main selector switch in position V-1 and adjust control V-1 so that meter pointer is exactly on the red mark at 60° point. This adjustment sets the value of vector voltage of Channel I to V_0 (see Chapter II). The automatic volume control of Channel I is now operating and is keeping the value of V_0 constant despite the variation of the magnitude of the input voltage to Channel I. The action of the automatic volume control is to preserve the magnitude of V_0 to within 5% for amplitude variations of the input voltage to Channel I of 26 db. Next, the gain of the inverter stage is checked by changing the position of toggle switch marked "SUM" and "DIFF" back and forth and observing the meter deflection. If the "DIFF" reading does not equal exactly to the "SUM" reading on the meter, the gain of the inverter stage is changed by turning screw driver adjustment marked "INVERTER ADJ." The main selector switch is then placed in V-2 position and the meter pointer is brought to the red mark by adjustment of knob marked V-2. Carrying these processes through as described above, two voltages of equal magnitude V_o are created and are substantially independent of the variation of the original voltages under test over the required frequency range. The main selector switch is placed next into "PHASE" position. The reading of the meter then represents phase angle difference in degrees between the input voltage to Channel I and input to Channel II of the Phase Meter. The SUM-DIFF switch is so positioned that the indicating meter pointer is on scale. If the switch is in the "DIFF" position, the difference scale of the meter is read. If the switch is in the "SUM" position, the sum scale is read. Improper switch position results in the meter pointer going off scale and can be brought back on scale by changing the position of SUM-DIFF switch. Improper position of this switch cannot damage the meter because of the overload characteristics of the final triode stage driving the full wave rectifier. The proper quadrant for phase angles is determined either from the consideration of the circuit under test either for very low or very high frequency, from resonance points at which phase angle is equal or nearly equal to zero, or by the Lissajous figures of a monitoring oscilloscope, if such is used, across the input terminals of Channels I and II.

To determine whether the phase angle is leading or lagging, a simple RC network may be inserted at the input of, say, Channel I, so arranged that the voltage across the resistor leads the voltage across the RC combination. If the meter reading increases, it means that the input voltage to Channel I was leading the input voltage to Channel II before the RC network was introduced. If the meter reading decreases, it means that the input voltage to Channel I was initially lagging the input voltage to Channel II.

CHAPTER V

Operation, Design, and Performance of the Component Portions of the Phase Shift Meter

For study and analysis purposes, the entire Phase Shift Meter circuit can be conveniently separated into several descrete portions as follows:

1. Automatic Volume Control Circuit.
2. Inverter Stage.
3. Mixer Stage.
4. Full Wave Rectifier Detector
5. Indicating Meter

Of these, the automatic volume controls are identical in the two channels comprising the meter, the inverter stage is inserted at will into Channel I and the remaining items are common to both channels.

1. Automatic Volume Control Circuit.

The automatic control circuit of either Channel I or Channel II consists of a variable gain pentode stage T_1 whose gain is varied by changing the value of the suppressor bias. The output of this stage is further amplified by two stage resistance-condenser coupled amplifiers T_3 and T_5. The output of T_5 is rectified by a

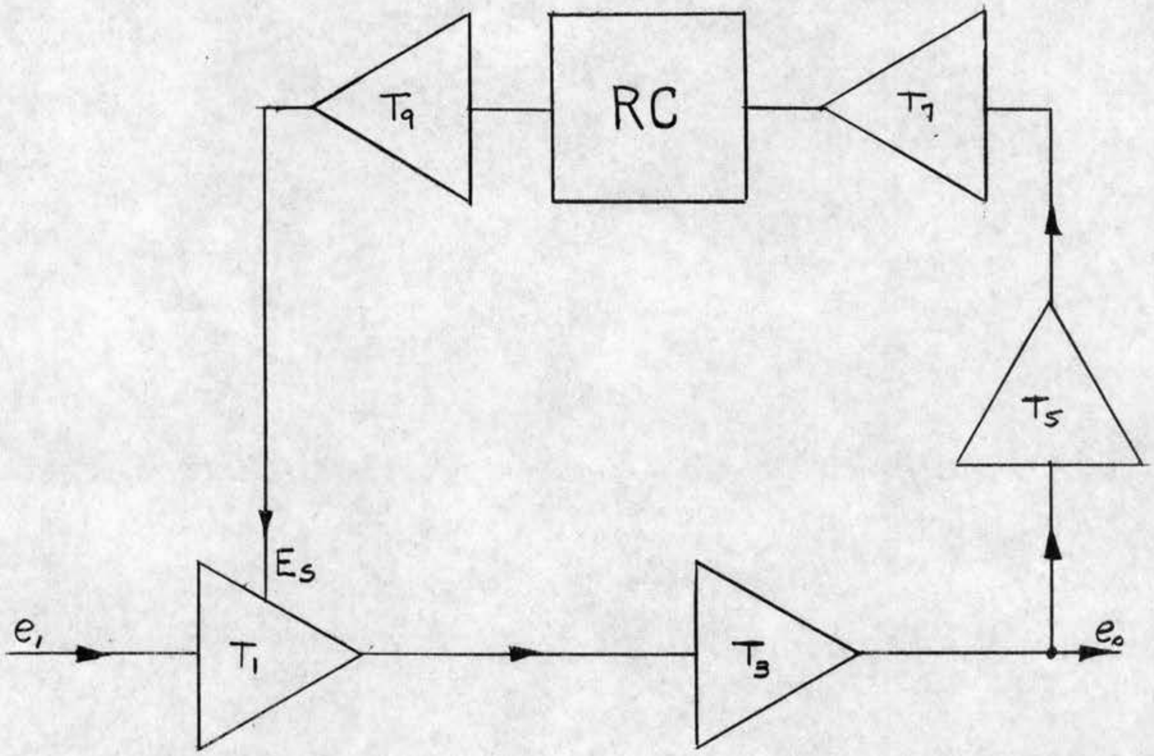

Figure 10. Schematic Block Diagram of the
Automatic Control Circuit.

half wave rectifier stage T_7 which is followed by an RC filter to smooth out the rectifier ripple. The d.c. voltage thus produced is further amplified by a stage of direct coupled amplifier T_9 and is then applied to the suppressor grid of stage T_1. The block diagram of this arrangement is shown in Figure 10 and the actual circuit in Figure 5. The controlled voltage is derived at the junction of stages T_3 and T_5. Thus the automatic control amplifier section proper consists of stages T_1 and T_3 and the negative feedback portion of the automatic control circuit consists of stages T_5, T_7, and T_9. The automatic volume control is identical in Channel II of the Phase Shift Meter.

In analyzing the action of this automatic volume control, certain voltage measurements were made to determine the gain of the various portions of the negative feedback circuit. The results of these measurements were then applied to the theoretical formulae describing the action of this control and the overall performance was computed. The computed performance was then compared to an actual control characteristic of the circuit.

Referring to Figure 10, it may be seen that for such a negative feedback circuit

$$e_o = \mu K_1 e_1 \qquad (8)$$

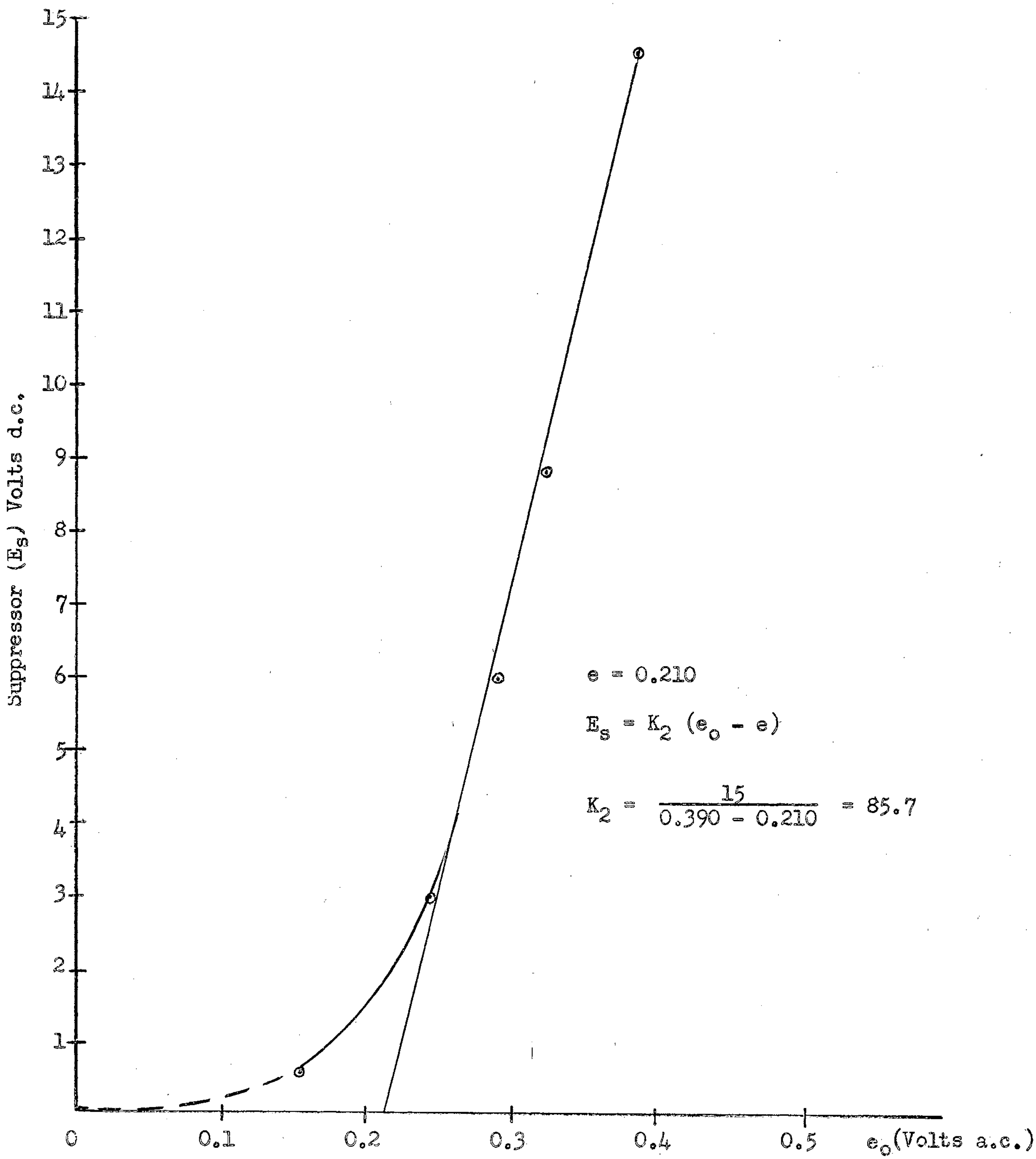

Figure 11. Suppressor Characteristic

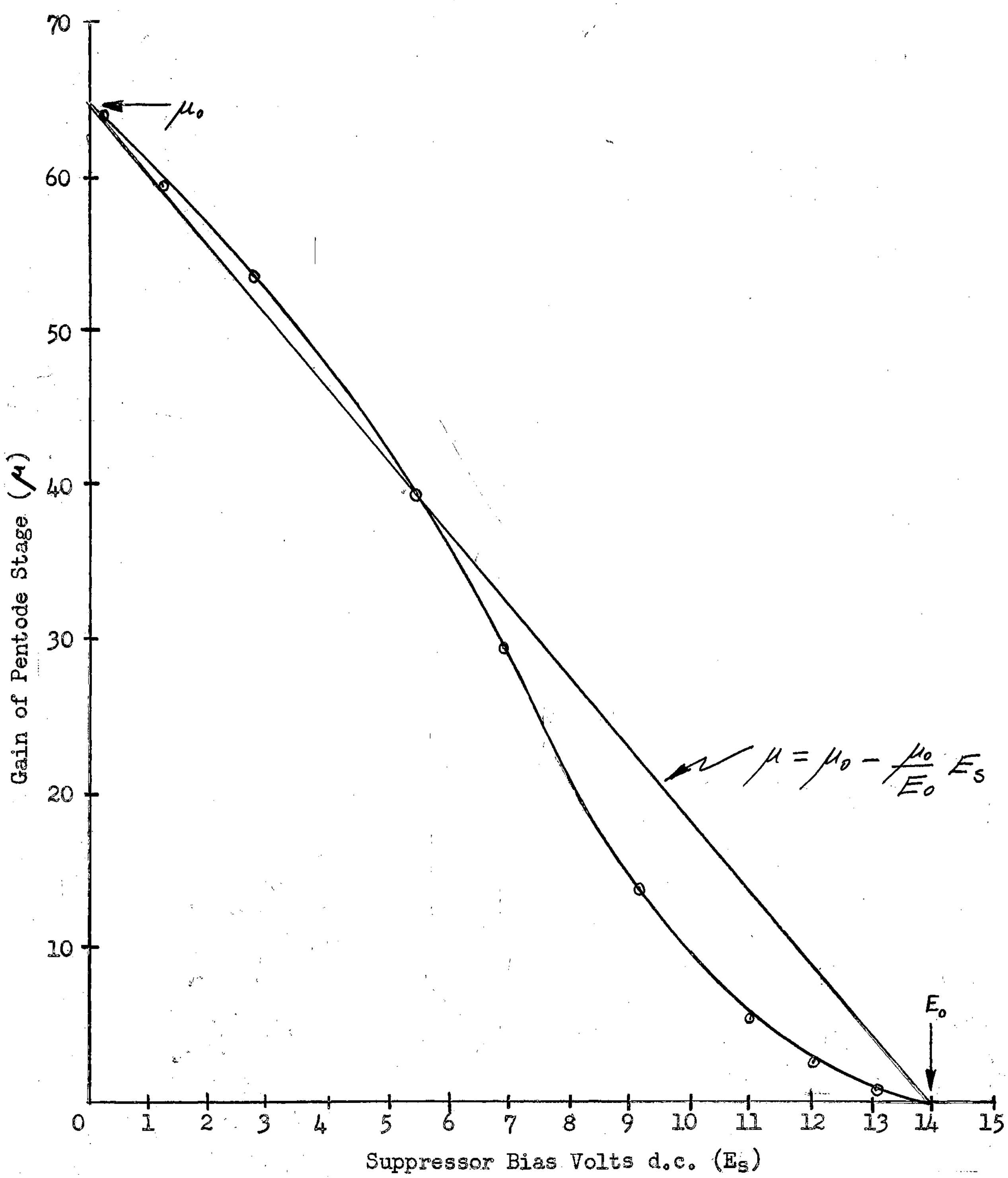

Figure 12. Gain Vs. Suppressor Bias

where e_o - output voltage

μ - variable gain of the pentode stage T_1

K_1 - gain of stage T_3

e_1 - input voltage.

From an actual measurement on the circuit, the following relation is established.

$$E_s = K_2 (e_o - e) \tag{9}$$

The plot of this relation is shown in Figure 11 which demonstrates the relationship between the suppressor bias E_s applied to pentode stage T_1 and the output voltage e_o. In this case e is the intercept of the characteristic on the abscissa. The method of obtaining this characteristic as well as the original data are given in Appendix A.

Another relation obtained experimentally is shown in Figure 12. This characteristic shows the variation of the gain of the pentode stage T_1 as a function of the suppressor bias E_s. The method of determining this characteristic and the original data are also given in Appendix A. The characteristic can be approximated mathematically by a relation

$$\mu = \mu_o - \frac{\mu_o}{E_o} E_s \tag{10}$$

where μ - gain of stage T_1

μ_o - gain of this stage with $E_s = 0$

E_o - suppressor bias necessary to produce zero gain of stage T_1.

Combining equations (8), (9), and (10)

$$e_o = K_1(\mu_o - \frac{\mu_o}{E_o} E_s)\, e_1$$

$$e_o = K_1 \left[\mu_o - \frac{\mu_o}{E_o} K_2\, e_o + \frac{\mu_o}{E_o}\, e\right] e_1$$

$$e_o = K_1 \mu_o\, e_1 - K_1 K_2 \frac{\mu_o}{E_o}\, e_o e_1 + K_1 K_2 \frac{\mu_o}{E_o}\, e e_1$$

From which

$$e_o = \frac{(K_1 \mu_o + K_1 K_2 \frac{\mu_o}{E_o} e)\, e_1}{1 + K_1 K_2 \frac{\mu_o}{E_o} e_o} \qquad (11)$$

From Figures 11 and 12, the various constants may be determined as follows:

$\mu_o = 65$; $E_o = 14$ volts; $e = 0.210$ volts.

$$K_2 = \frac{15}{0.385 - 0.210} = 85.7 \text{ dc volts/a.c. volts}$$

$K_1 = 11.9$ by separate measurement of gain of stage T_3.

By substituting the above constants into equation (11), the following relation is obtained

$$e_o = \frac{1775 e_1}{1 + 4750 e_1} \qquad (12)$$

which relates the controlled voltage e_o to the input voltage e_1.

Equation 12 is converted in decibel form such that e_1 is plotted in db below 100 millivolts which is the maximum input signal tolerated by each channel of the Phase Shift

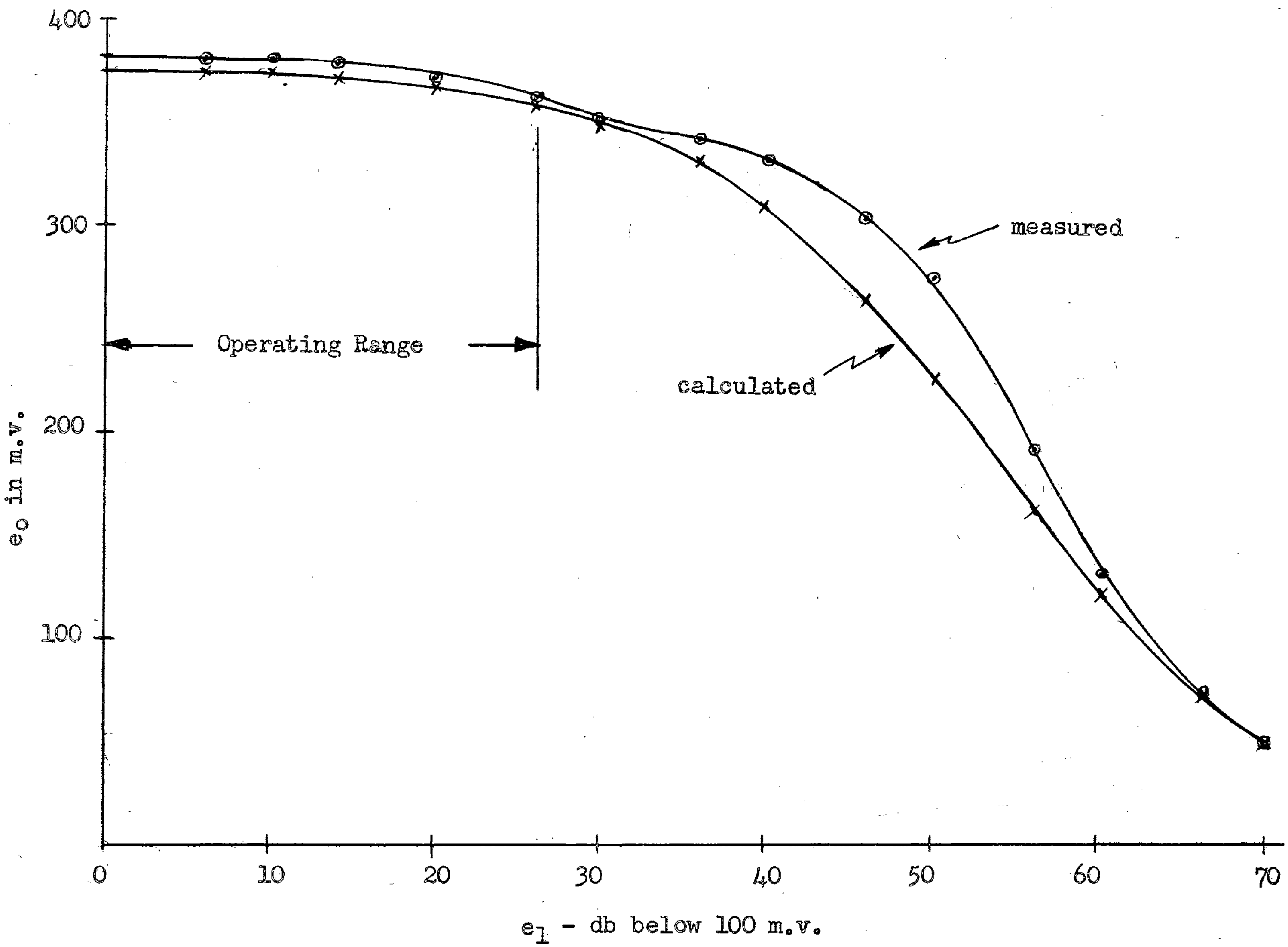

Figure 13. Calculated and Measured A.V.C. Characteristic.

Meter, so that

$$db = 20 \log_{10} \frac{e_1}{100} \qquad (13)$$

values of e_1 being selected in millivolts.

The plot of equation (12) on the above basis is shown in Figure 13. The actual measured control characteristic obtained with the automatic volume control circuit is also plotted in Figure 13. The calculations and measurement data are included in the Appendix A. The comparison of the computed and measured characteristics shows a good correspondence indicating correctness of the analysis of the negative feedback circuitry. The discrepancy between the two curves is caused by the departure of e_o Vs. E_s characteristic from the assumed straight line. From these plots, it may be seen that the automatic volume control preserves the magnitude of e_o (and therefore V_o) to about 5% within the range of variation of the input voltage from zero to 26 db below 100 millivolts. This control characteristic was found to be adequate in normal type of phase measurement on filters and other types of networks where the amplitude variations from the peak of the filter response characteristic is of the order of ten or twenty to one.

2. Inverter Stage.

The inverter stage of the Phase Shift Meter is designed to have gain of exactly unity. Its purpose is to invert the phase of voltage V_1 after the latter has been adjusted to the magnitude

V_o by the action of the automatic volume control described in the preceding section. The circuit comprising this stage is given in Figure 5 and consists of tube T_{11} having an unbypassed cathode and a tapped plate resistors.

In designing such a stage, the following analysis is used:

If e_1 - input voltage to the stage

e - voltage grid to cathode

e_o - output voltage

μ - amplification factor of the tube

R_c - cathode bias resistor

$R_1 + R_2$ - total plate load resistance

R_2 - Resistor across which e_o is derived

then

$$e = e_1 - i R_c \qquad (14)$$

$$i = \frac{\mu e}{R_1 + R_2 + R_c} \qquad (15)$$

$$e_o = i R_2 \qquad (16)$$

These relations are evident from Figure 14

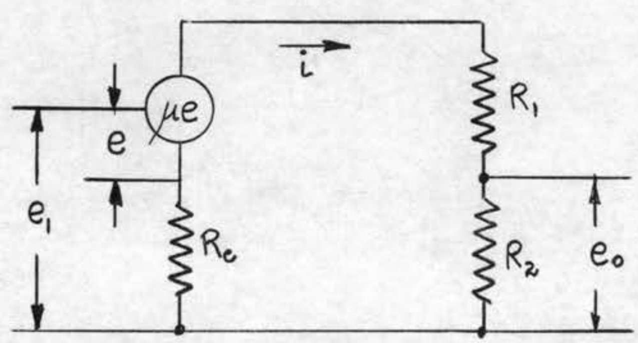

Figure 14. Equivalent Circuit of the Inverter Stage.

From equations (14), (15), and (16)

$$e_o \left[R_1 + R_2 + (1 + \mu) R_c\right] = \mu e_1 R_2 \qquad (17)$$

If it desired to make $\frac{e_o}{e_1} = 1$,

Then

$$\frac{\mu R_2}{R_1 + R_2 + (1 + \mu) R_c} = 1 \qquad (18)$$

and

$$R_c = \frac{(\mu - 1) R_2 - R_1}{1 + \mu} \qquad (19)$$

If we choose to make R_1 = 100 K ohms and R_2 = 25 K ohms and for the type of tube used $\mu = 36$, then the value of R_c becomes, using equation (19)

$$R_c = \frac{(36-1) \times 25{,}000 - 100{,}000}{36 + 1} = 21\text{K ohms} \qquad (20)$$

In order to allow some adjustment of the stage gain, the cathode resistor is made up of fixed 15K resistor and a variable 10K resistor. This adjustment is effected through the front panel of the instrument by means of a screw driver. This stage is removed from the circuit by means of switch S_o (see Figure 5).

3. Mixer Stage.

This stage consists of two triode sections T_{12} and T_{14} (see Figure 5) which have a common plate load resistor. It serves to add algebraically the outputs of the automatic volume controls of Channel I and II after the input voltages V_1 and V_2 have been adjusted to value V_o.

The equivalent circuit of the mixer stage is shown in Figure 15.

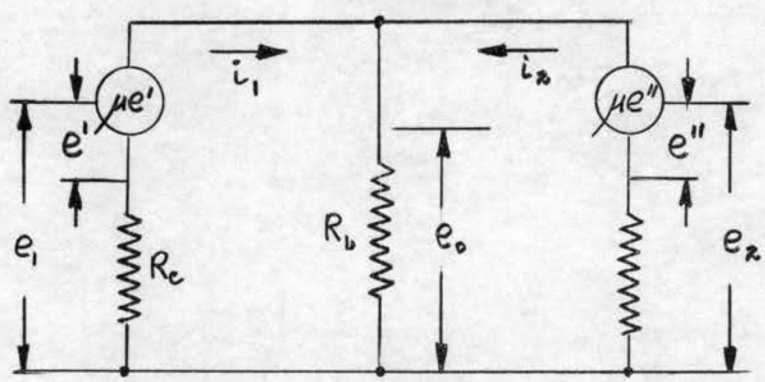

Figure 15. Equivalent Circuit of the Mixer Stage.

If e_1 and e_2 are two input voltages to be added,

R_L - common plate resistor,

R_c - individual cathode bias resistors,

e_o - output voltage across resistor R_L,

e' - grid to cathode voltage of tube T_{12},

e'' - grid to cathode voltage of tube T_{14},

μ - amplification factor of tubes T_{12} and T_{14}

then

$$e_o = R_L\,(i_1 + i_2) \tag{21}$$

$$e' = e_1 - i_1 R_c; \quad e'' = e_2 - i_2 R_c \tag{22}$$

$$(i_1 + i_2)\,R_L + i_1 R_c = \mu e' \tag{23}$$

$$(i_1 + i_2)\, R_L + i_2 R_c = \mu e'' \tag{24}$$

Adding equations (23) and (24) and substituting (22),

$$2R_L\,(i_1 + i_2) + R_c\,(i_1 + i_2) = \mu(e_1 - i_1 R_c) + \mu\,(e_2 - i_2 R_c) \tag{25}$$

Substituting equation (21) into equation (25) and reducing,

$$e_o = \frac{\mu R_L\,(e_1 + e_2)}{2R_L + R_c\,(1 + \mu)} \tag{26}$$

If we choose R_L = 100K R_c = 5K and $\mu = 36$

$$e_o = \frac{36 \times 100{,}000\,(e_1 + e_2)}{200{,}000 + 5{,}000\,(1 + 36)} = 9.3\,(e_1 + e_2) \tag{27}$$

From equation (27) it is at once evident that the output voltage e_o is the sum of the two input voltages e_1 and e_2. The net voltage gain of this stage is 9.3. Actual gain, as measured, is 10.0.

4. Full Wave Rectifier Detector and Indicating Meter.

Having obtained at the output of the mixer stage either V_{SUM} or V_{DIFF} vector, the magnitude of which is a function of the phase angle, the next step is to provide a meter indication which reads directly in degrees phase. This is achieved by further amplification of the mixer stage output by means of driver stage T_{15} (see Figure 5) which feeds a full wave rectifier circuit consisting of two resistors R_{29} and R_{29} and two half wave rectifiers T_{17} and T_{18} connected in a bridge circuit. A d.c. microammeter is connected between the junction of resistors R_{29} and R_{29} and joined cathodes of tubes T_{17} and T_{18}. Diagram of this bridge is shown in Figure 16.

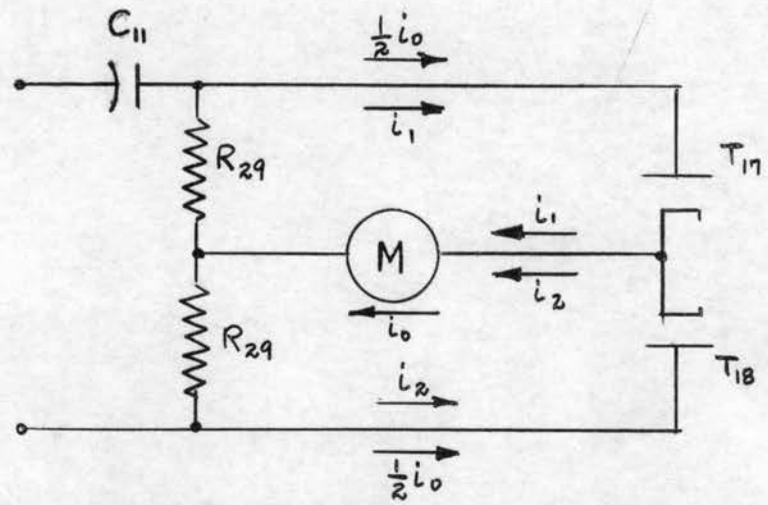

Figure 16. Detector Circuit of the Phase Shift Meter.

To enable coupling of the rectifier circuit to the driver stage by a condenser-resistance network, one corner of the bridge is at ground potential. The meter itself is, therefore, above ground.

If a sinusoidal voltage is applied across resistors R_{29} and R_{29}, current i_1 flows through meter M during the half cycle in the direction shown when the instantaneous voltage is positive with respect to ground. Current i_2 flows through the meter M during the half cycle when the voltage across R_{29} R_{29} is negative with respect to ground. In addition to currents i_1 and i_2, current i_o flows through the meter due to the contact potential of rectifier tubes T_{17} and T_{18}. Normally the zero of the meter is mechanically depressed so that the pointer is on zero when no a.c. voltage is applied across R_{29} and R_{29}. The meter reads the average value of rectified sinusoidal currents i_1 and i_2.

For the case of sinusoidal input to the bridge $i_1 = i_2$ in magnitude. Then

$$i_{av.} = \frac{2}{T} \int_0^{\frac{T}{2}} I \sin \frac{2\pi}{T} t \, dt \tag{28}$$

where I is the maximum value of current and T is the period of the sine wave input

$$i_{av.} = \frac{2}{T} \left[-\frac{IT}{2\pi} \cos \frac{2\pi}{T} t \right]_0^{\frac{T}{2}} = \frac{2I}{\pi} \tag{29}$$

If E_{in} is the r.m.s. value of voltage input across resistors R_{29} and R_{29}, then $E_{max} = \sqrt{2} \; E_{in}$

$$I = \frac{\sqrt{2} \; E_{in}}{R_{29} + 2R_m + 2R_r} \tag{30}$$

where R_M - resistance of the meter

R_r - forward resistance of the rectifier.

In this design $R_{29} > 2R_M + 2R_r$ and therefore from equations (29) and (30)

$$i_{av.} = \frac{2\sqrt{2} \; E_{in}}{\pi R_{29}} \tag{31}$$

Since $R_{29} = 2.5 \times 10^5$ ohms, theoretical ratio of $\frac{i_{av.}}{E_{in}}$

$$= \frac{2 \sqrt{2} \ 10^6}{\pi \times 2.5 \times 10^5}$$

$= 3.6$ microamperes/volt a.c.

The measured ratio of $\frac{i_{av.}}{E_{in}} = 3.4$ microamperes/volt a.c.

CHAPTER VI

Calibration of the Phase Shift Meter

The calibration of the Phase Shift Meter can be most readily carried out by using a simple RC network shown in Figure 17. The purpose of the calibration is to prepare a meter scale which reads directly in degrees phase. Since the detector response departs slightly from linearity and moreover includes quiescent diode current, the meter scale (in degrees) departs slightly from a theoretical conversion scale computed on the basis of equations (4) and (7).

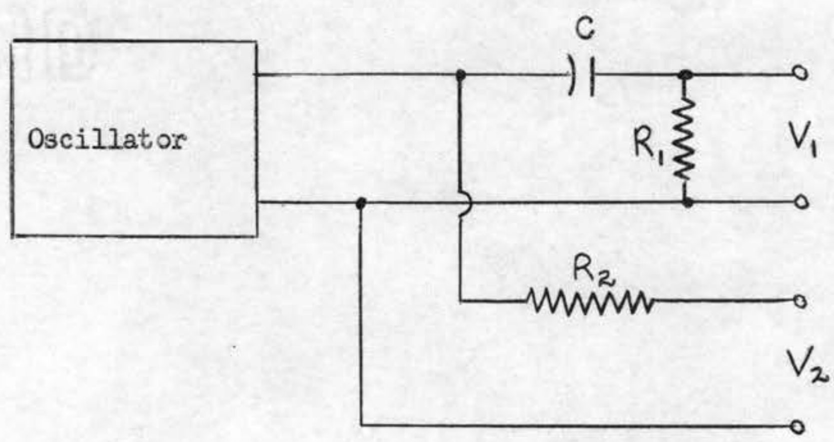

Figure 17. RC Circuit Used for Calibrating the Phase Shift Meter.

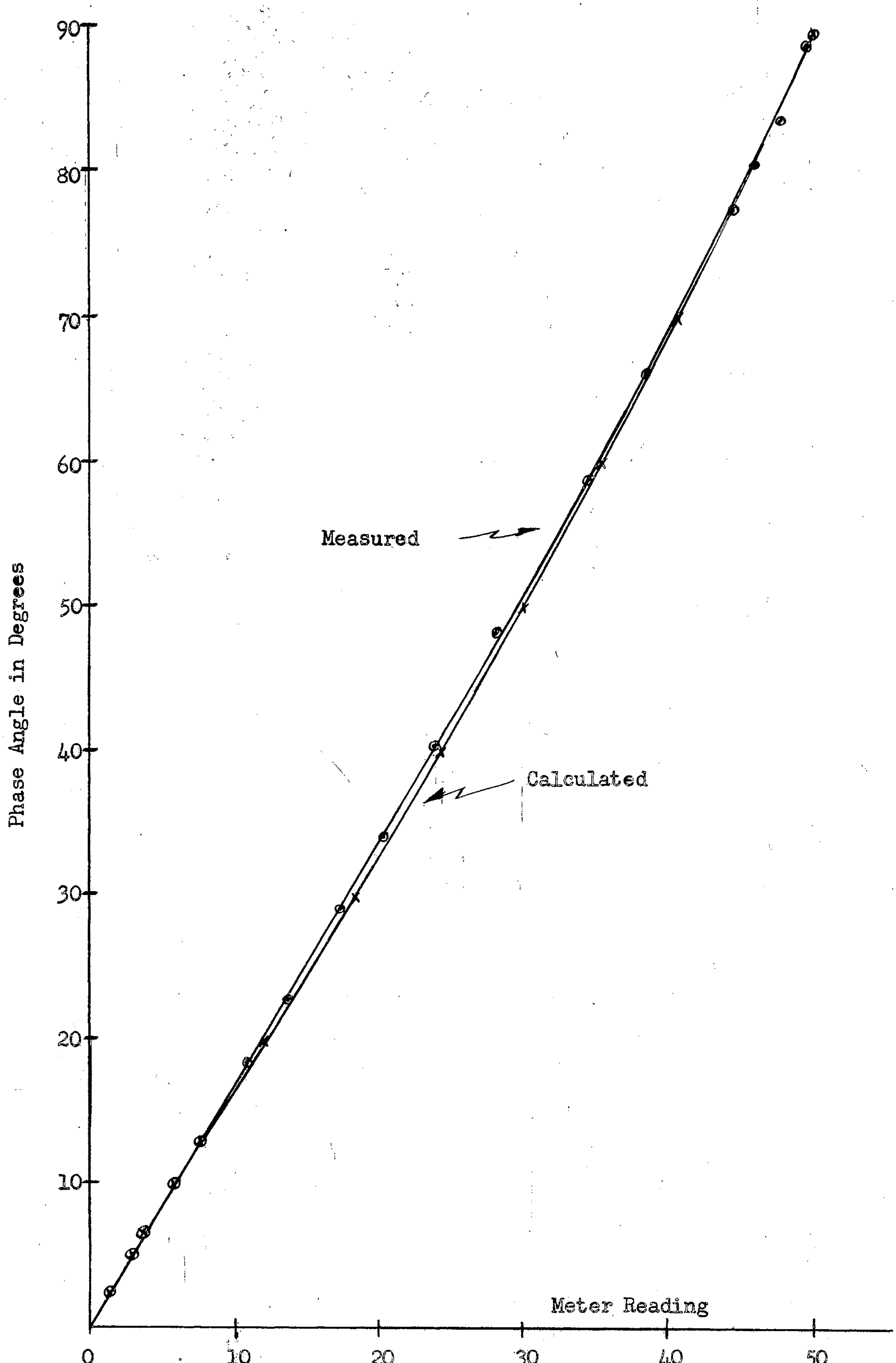

Figure 18. Calibration of the Indicating Meter.

The meter scale is calibrated at a fixed frequency. The value of the phase angle is varied by shifting the value of condenser C of Figure 17. Since the generator impedance is much less than the value of resistances R_1 and R_2 chosen, the phase difference θ between input V_1 and V_2 is given by

$$\theta = \tan^{-1} \frac{1}{R_1 \omega C} \tag{32}$$

In carrying out the calibration, each vector voltage V_o is adjusted to read 35 microamperes on the scale of a 50 microampere d.c. meter which prior to the measurement was depressed to read zero with both input voltages V_1 and V_2 set to zero. The theoretical and actual calibration curves are shown in Figure 18. It may be noted that the maximum departure between the two curves for a given angle θ amounts to 0.5 microamperes. Using the experimentally determined angle to microampere conversion, a meter scale was engraved which has been shown in Figure 9. Since the readings of the meter scale are dependent only on the settings of V_o, the calibration is quite stable and theoretically depends only upon the characteristic of the bridge detector driving the meter. Since the value of resistors R_{29} and R_{29} is large, experience has shown that no recalibration of the meter scale was ever necessary. The calculated and measured values of θ Vs. meter current are given in Appendix B.

CHAPTER VII

Performance of the Phase Shift Meter

In evaluating the performance of the present design of the Phase Shift Meter, it was deemed desirable to present an example of phase shift measurement on a network whose phase characteristic could be readily calculated. The comparison between the calculated and measured phase characteristic could then be made. Consequently, a simple antiresonant network was built up from available circuit components, as shown in Figure 19. To facilitate the measurement, the network was connected to an audio oscillator through a high resistance. This resistance was then considered

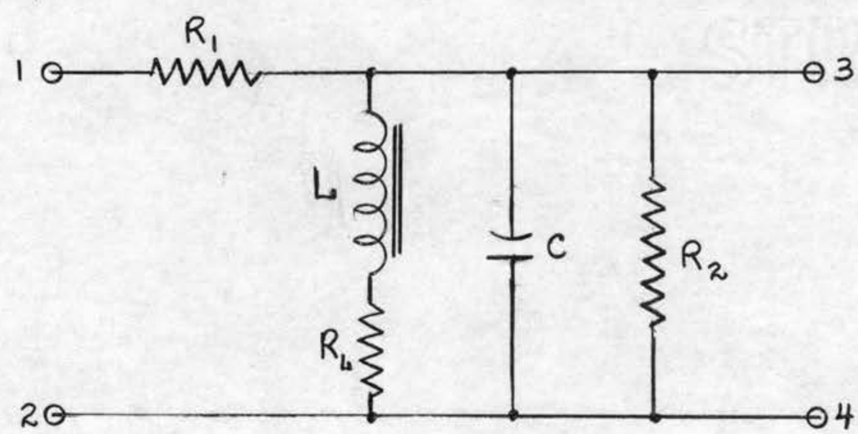

Figure 19. Circuit Diagram of a Simple Antiresonant Network.

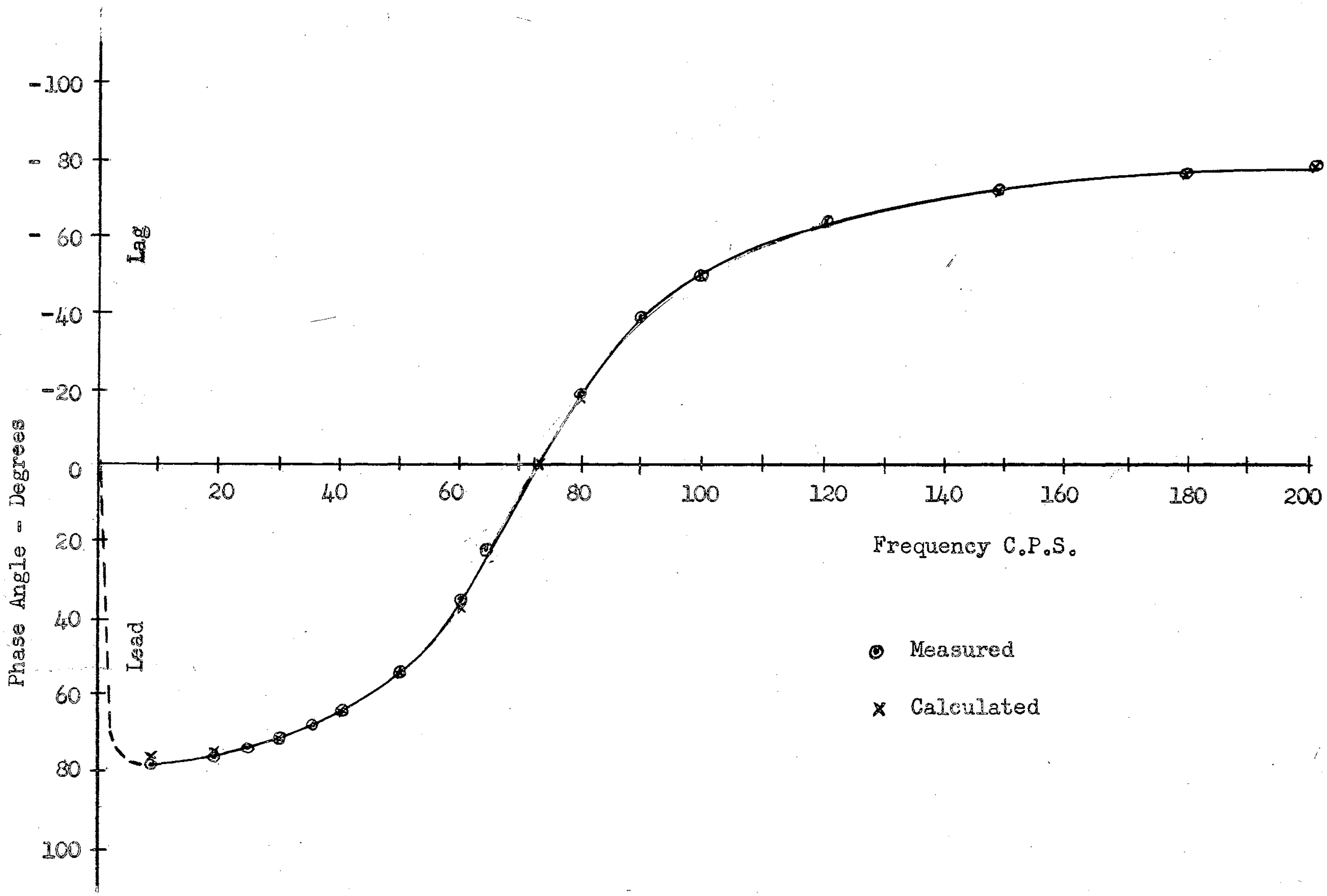

Figure 20. Phase Shift Characteristic of Antiresonant Network.

as a part of the network. The phase shift of this four-terminal network was determined by connecting Channel I of the Phase Shift Meter across terminals 1 and 2 and Channel II of the Phase Shift Meter across terminals 3 and 4. Obviously the connections between Channels I and II could have been interchanged without affecting the results. The frequency of the oscillator was varied in discrete steps from 10 c.p.s. to 200 c.p.s. and the phase angle between the input and the output of the network determined according to the operational procedure described in Chapter IV. As was pointed out previously, care was taken to connect terminals 2 and 4 which constitute the common bus of the network to each of the lower binding posts of the meter input, marked ground. The phase shift characteristic of the network as a function of driving frequency is shown in Figure 20. It may be noted that for frequencies approaching zero, the phase shift between input and output approaches zero since the capacitive reactance is high and voltage across the effective resistance of the choke is in phase with the current through it. At high frequencies the inductive reactance is high and the voltage across the capacitance lags the current through it by $\frac{\pi}{2}$. Since a high resistance is connected in series with the antiresonant portion of the network, the oscillator voltage is essentially in phase with the current through the capacitive reactance. At resonance, the phase characteristic goes through zero. The data used in plotting this phase shift characteristic is given in the Appendix C. In order to obviate a possible ambiguity in the choice of the phase angle quadrant, the frequency for which the phase shift was zero was determined and the oscillator setting was shifted first toward the low frequency end and then toward the high frequency end of the spectrum.

In order to compare the measured phase shift characteristic of the antiresonant circuit of Figure 19 to the theoretical phase shift characteristic, the following relations were derived:

The expression for the three complex impedances in parallel may be written as

$$Z_{34} = \frac{\frac{1}{j\omega C}(j\omega L + R_L) R_2}{\frac{1}{j\omega C}(j\omega L + R_L) + (j\omega L + R_L) R_2 + \frac{1}{j\omega C} R_2} \qquad (33)$$

The ratio of voltage <u>in</u> e_1 to voltage <u>out</u> e_2

$$\frac{e_2}{e_1} = \frac{Z_{34}}{R_1 + Z_{34}}$$

$$\frac{e_2}{e_1} = \frac{(j\omega L + R_L) R_2}{R_1(j\omega L + R_L) + j\omega C\, R_1 R_2 (j\omega L + R_L) + R_1 R_2 + (j\omega L + R_L) R_2} \qquad (34)$$

Rationalizing and taking the ratio of imaginaries to reals,

$$\theta = \tan^{-1} \frac{\omega L\, R_1 R_2 - \omega^3 L^2 C\, R_1 R_2 - \omega C R_1 R_L{}^2 R_2}{R_1 R_L R_2 + \omega^2 L^2 R_1 + \omega^2 L^2 R_2} \qquad (35)$$

Since $R_1 > R_2 > R_L$

$$\theta = \tan^{-1} \frac{R_2(\omega L - \omega^3 L^2 C - \omega C R_L{}^2)}{R_2 R_L + \omega^2 L^2} \qquad (36)$$

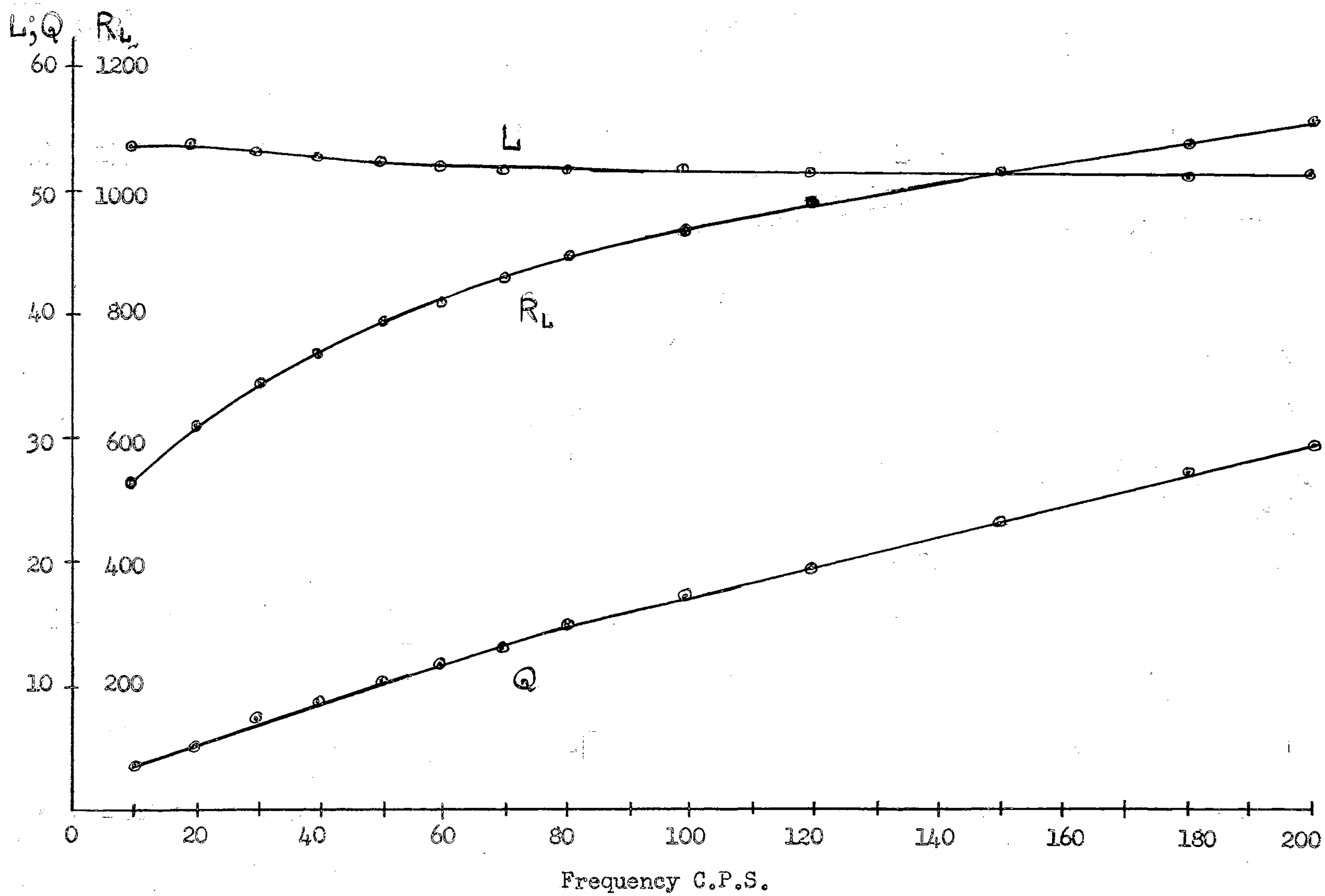

Figure 21. Variation of L, R_L and Q of the Choke with Frequency

The calculation of θ as a function of ω is also given in Appendix C. In calculating the phase characteristic, the variation of the inductance and effective resistance of the choke with frequency was taken into account. Experimentally determined variation of inductance, effective resistance and Q of the choke is shown in Figure 21, and the data is given in Appendix C. The calculated phase shift characteristic of the given network in Figure 20. It may be seen that the agreement is quite good. This example demonstrates the performance of the meter over a substantial frequency spectrum. It may be noted that, in general, phase measurements become more difficult as the frequency approaches zero. At very high frequencies effects of distributed capacities of networks under measurement likewise pose a problem.

The intrinsic design of the phase meter is such that the device should be capable of measuring the difference in phase angles of two sinusoidal voltages over a wide frequency spectrum. This theoretical independence with respect to the frequency range can be realized if the two channels involving automatic volume control, the various amplifying stages and the phase inverter have the identical phase characteristic over the desired frequency band. In other words, the phase shift of either channel need not necessarily be zero over the specified frequency range. In a practical case, however, there is an upper frequency limit beyond which the instrument does not indicate the correct phase angle. This is due to the presence of distributed capacity in the switches and wiring, particularly in the phase inverter stage which is either inserted or removed from the circuit. In the present design the upper frequency limit of operation is about 2000 c.p.s. This is determined in the following way: The method consists of feeding the same voltage into Channel I and II simultaneously and observing the deflection of the meter on the "difference" scale. This remains zero so long as the differential phase shift of the two Phase Shift Meter channels remains zero. A finite angle is indicated on the meter when this frequency range is exceeded. Since in its present form of the meter is designed for use in the sub-audio range, the upper frequency limit of 2000 c.p.s. is considered adequate. Obviously the operating frequency range of the instrument can be increased greatly by proper attention to the design of coupling circuits, impedances, wiring and switching. The present meter can handle input voltages of several tens of volts down to about 10 millivolt r.m.s. By using proper input attenuators the signal handling capacity can be greatly increased.

CHAPTER VIII

Summary and Conclusions

The measurement of phase angle is considered to be an important adjunct to the determination of the steady state behavior of electrical networks and electrical apparatus. This quantity can be easily determined by the instrument treated in this Thesis. The principle of operation, various design factors and the performance of the Phase Shift Meter are treated at length. The operation of the Phase Shift Meter is based upon the measurement of the magnitude of the resultant difference or sum vector which is derived from two other vectors representing the two sinusoidal input signals having an unknown phase angle difference. The two vectors representing the input signals are each equalized to a predetermined magnitude by the action of a precise automatic volume control. Theoretical and actual performance of this control are discussed at length. The performance of the Phase Shift Meter is illustrated by an actual measurement of phase shift of an antiresonant network and this is compared to a theoretically derived characteristic. The methods of calibration and operation are likewise presented.

As the result of the development and the evaluation of the various design factors and performance of the Phase Shift Meter, it may be concluded that this instrument can serve very adequately in carrying phase shift determinations on a variety of electrical or electromechanical devices. While in its present design it is capable of measuring phase shift in the sub-audio and lower audio range, its performance can be relatively easily extended to encompass the higher frequency spectrum. The instrument has proven to be reliable and convenient to use in the laboratory as well as in the field. Through its application as a measuring device, many difficult design problems encountered in electronic and electromechanical instrumentation research and development have been carried to a successful solution.

BIBLIOGRAPHY

Arguimbau, L. B. Vacuum Tube Circuits. New York: John Wiley and Sons, 1948.

Bode, H. W. Network Analysis and Feedback Amplifier Design. New York: D. Van Nostrand Company, 1945.

Brown, G. S. and Campbell, D. P. Principles of Servomechanisms. New York: John Wiley and Sons, 1948.

Bush, V. Operational Circuit Analysis. New York: John Wiley and Sons, 1929.

Everitt, W. L. Communication Engineering. New York: McGraw-Hill Book Company, 1932.

Glaser, J. L. "Accurate Phase Difference by Lissajous Figures" Electronics II (March 1952).

Goldman, S. Transformation Calculus and Electrical Transients. New York: Prentice Hall 1949.

Guillemin, E. A. Communication Networks. Vol. I and II. New York: John Wiley and Sons, 1931.

Laws, F. A. Electrical Measurements. New York: McGraw-Hill Book Company, 1917.

Manley, R. G. Waveform Analysis. New York: John Wiley and Sons, 1945.

McLean, W. R. and Sivian, L. V. "Direct Reading Audio Phase Meter." Journal of the Acoustical Society of America. 25 (April, 1931).

Nyquist, H. and Brand, S. "Measurement of Phase Distortion" The Bell System Technical Journal IX (July, 1930).

Pender, H. and McIlwain, K. Electrical Engineering Handbook (Electrical Communication and Electronics) Fourth Edition. New York: John Wiley and Sons, 1950.

Terman, F. E. and Pettit, J. M. Electronic Measurements. Second Edition. New York: McGraw-Hill, 1952.

APPENDIX A

Suppressor Characteristic

This characteristic was obtained by opening the negative feedback between stages T_1 and T_3, applying variable voltage to the grid of T_3 at constant frequency (100 c.p.s.) and measuring voltages e_o and E_s (see Figure 10).

e_o Volts a.c.	E_s Volts d.c.
0.385	-14.5
0.320	- 8.8
0.290	- 6.0
0.245	- 3.0
0.155	- 0.6

APPENDIX A
(Continued)

Gain Vs. Suppressor Bias

This characteristic was obtained by applying a fixed frequency a.c. signal (100 c.p.s.) to the control grid of either T_1 or T_2 (6J7 pentode). The r.m.s. voltage input e_{in} = 0.015 volts. Variable negative bias E_s was applied to the suppressor grid and voltage output e_o across load resistor was measured.

$$\text{Gain} = \frac{e_o}{e_{in}}$$

E_s Volts	e_o Volts	Gain
0	1.00	66.6
-1.5	0.91	60.6
-3.0	0.82	54.7
-4.5	0.70	46.7
-6.0	0.56	37.4
-7.5	0.39	26.0
-9.0	0.22	14.6
-10.5	0.08	5.3
-12.0	0.023	1.5
-13.5	0	0

APPENDIX A
(Continued)

Calculation of the A.V.C. Characteristic

$$e_o = \frac{1775e_1}{1 + 4750e_1}$$

e_1 Volts	db below 100 m.v.	e_o Volts
0.100	0	0.374
0.050	6	0.374
0.0316	10	0.374
0.020	14	0.371
0.010	20	0.366
0.005	26	0.359
0.00316	30	0.350
0.00158	36	0.330
0.00100	40	0.309
0.0005	46	0.263
0.000316	50	0.224
0.000158	56	0.160
0.000100	60	0.120
0.0000316	70	0.049

APPENDIX A
(Continued)

Measurement of the A.V.C. Characteristic

Input voltage to grid either T_1 or T_2 = 0.100 volt. Frequency = 100 c.p.s. A db "T" pad attenuator inserted at the input. Voltage e_o (see Figure 10) is measured for various values of the input voltage to the grid.

db below 100 m.v.	e_o Volts	db below 100 m.v.	e_o Volts
0	0.380	40	0.330
6	0.380	46	0.303
10	0.380	50	0.275
14	0.378	56	0.190
20	0.370	60	0.128
26	0.360	66	0.069
30	0.350	70	0.045
36	0.340		

APPENDIX B

Calibration of the Phase Shift Meter

$R_1 = 10^4$ ohms; $R_2 = 2 \times 10^6$ ohms   f = 45.0 c.p.s.

Meter depressed mechanically to zero for $V_1 = V_2 = 0$

C mfd	$\frac{1}{R_1 WC}$	θ Degrees	Meter Reading Microamperes
0.0022	161.9	89.7	49.8
0.0100	35.4	88.4	49.5
0.0389	9.10	83.8	47.6
0.0586	6.04	80.6	46.1
0.0778	4.55	77.6	44.5
0.1556	2.28	66.3	38.4
0.2119	1.67	59.1	34.6
0.3182	1.11	48.1	28.3
0.4173	0.849	40.4	23.9
0.5282	0.677	34.1	20.3
0.6291	0.563	29.4	17.5
0.8414	0.421	22.9	13.6
1.053	0.336	18.6	11.1
1.530	0.232	13.1	7.7
1.992	0.178	10.1	5.9
3.038	0.116	6.7	3.9
4.015	0.088	5.1	3.0
8.058	0.044	2.5	1.5
∞	0	0	0

APPENDIX C

Measured Phase Shift Characteristic of an Antiresonant Network

Frequency c.p.s.	Phase Shift Angle Degrees
10	+79.0 (lead)
20	+76.0
25	+73.5
30	+71.0
35	+67.5
40	+64.0
50	+53.0
60	+34.0
65	+20.5
72.5	0
80	-19.0 (lag)
90	-38.5
100	-50.5
120	-63.0
150	-71.0
180	-76.0
200	-78.0

APPENDIX C
(Continued)

Calculations of the Phase Shift Characteristic of an Antiresonant Network

$$\theta = \tan^{-1} \frac{R_2 \left(\omega L - \omega^3 L^2 C - \omega C R_L^2\right)}{R_L R_2 + \omega^2 L^2}$$

R_2 = 47,600 ohms   C = 0.0897 mfd.

f	ω	ωL	$\omega^2 L^2$	ωC	$\omega^3 L^2 C$	tan	θ	
10	62.8	3,360	1.13 X 10^7	56.3 X 10^7	63.5	4.30	+ 77.0	(Lead)
20	126	6,760	4.58	113	516	3.96	+ 75.8	
30	188	10,100	10.2	168	1,710	2.96	+ 71.4	
40	252	13,400	18.0	226	4,070	2.07	+ 64.2	
50	314	16,600	27.6	282	7,800	1.34	+ 53.2	
60	377	19,800	39.0	338	13,200	0.735	+ 36.3	
73	457	23,900	57.1	409	23,600	0	0	
80	503	26,200	68.5	452	31,000	-0.315	- 17.5	(Lag)
100	628	32,500	106	563	59,600	-1.18	- 49.6	
120	754	39,000	152	676	102,500	-1.94	- 62.7	
150	940	48,200	233	845	197,000	-2.99	- 71.5	
180	1130	58,000	366	1010	370,000	-4.00	- 76.0	
200	1256	64,500	415	1130	470,000	-4.60	- 77.8	

APPENDIX C
(Continued)

Measured Inductance and Effective Resistance of a Choke as a Function of Frequency

Measurements made using Owen Bridge

$L = ASC_u \qquad R_L = \frac{C_u}{C_a} S - B \qquad Q = \frac{\omega L}{R_L}$

$S = 10^4$ ohms; Cu = 1 mfd. C_a = 9 mfd.

f cps	A ohms	B ohms	L henries	R_L ohms	Q
10	5350	580	53.5	530	6.35
20	5360	490	53.6	620	10.8
30	5340	420	53.4	690	14.5
40	5306	370	53.1	740	17.8
50	5276	320	52.8	790	21.0
60	5250	290	52.5	820	24.1
70	5230	240	52.3	860	26.4
80	5211	220	52.1	890	29.5
100	5186	170	51.9	940	34.6
120	5167	130	51.7	980	39.8
150	5145	60	51.5	1030	47.0
180	5137	30	51.4	1070	54.3
200	5130	0	51.3	1110	58.0

VITA

Joseph D. Eisler
candidate for the degree of
Master of Science

Thesis: A PHASE SHIFT METER, ITS DESIGN AND PERFORMANCE.

Major: Electrical Engineering.

Biographical and Other Items:

Born: September 19, 1909 at Moscow, Russia.
U. S. Citizenship 1938.

Undergraduate Study: Massachusetts Institute of Technology, 1932. B.S. in Electrical Engineering.

Graduate Study: Massachusetts Institute of Technology, 1934. Oklahoma Agricultural and Mechanical College, 1950-54.

Experience: Research on Thompson Effect in Metals, M.I.T. 1932-34; Development of Seismographs, M.I.T. 1934-35. Research and Development Geophysical and Electronic Instrumentation, Stanolind Oil and Gas Company 1936-42; Research in Aircraft to Aircraft Fire Control, the Franklin Institute, Philadelphia, Penn., 1942-44; Applied and Fundamental Geophysical Research, Stanolind Oil and Gas Company, Tulsa, Oklahoma, 1944-. Now Research Section Supervisor, Research Department, Stanolind Oil and Gas Company, Tulsa, Oklahoma.

Senior Member: The Institute of Radio Engineers.

Member: Society of Exploration Geophysicists, Seismological Society of America, and American Geophysical Union.

Associate Member: The Society of Sigma Xi.

Holder of a number of patents in the fields of Geophysics and Instrumentation.

Author and Co-author of published articles as follows:

1. "Precise Speed Control for D.C. Machines" (with R. H. Frazier and W. P. Frantz), Electrical Engineering 54 No. 3, March, 1935.

VITA
(Continued)

2. "Multichannel Pen Recorder for Electrical Logging Operations" (with D. Silverman) Geophysics XII No. 3, July, 1947.

3. "Vehicle Borne Instrument for Continuously Indicating Road Elevations" (with D. Silverman and J. F. Evans), Geophysics XII No. 3, July, 1947.

4. "A study of the Influence of Background Noise on Reflection Picking" (with K. Dyk) Geophysics XVI No. 3, July, 1951.

5. "An Automatically Recording Magnetic Balance" (with G. R. Newton and W. A. Adcock) The Review of Scientific Instruments 23 No. 1, January, 1952.

6. "Studies of a Surface Seismic Distrubance" Geophysics XVII No. 3, July, 1952.

THESIS TITLE: A Phase Shift Meter, Its Design and Performance.

AUTHOR: Joseph D. Eisler.

THESIS ADVISER: Professor Herbert L. Jones.

The content and form have been checked and approved by the author and thesis adviser. Changes or corrections in the thesis are not made by the Graduate School office or by any committee. The copies are sent to the bindery just as they are approved by the author and faculty adviser.

TYPIST: Margaret H. Todd